Element transport from slab to volcanic front at the Mariana arc

Elliott, T.R.; Plank, T.; Zindler, A.; White, W.; Bourdon, B.

published in
Journal of Geophysical Research. Solid Earth
1997

DOI (link to publisher)
10.1029/97JB00788

document version
Publisher's PDF, also known as Version of record

JOURNAL OF GEOPHYSICAL RESEARCH, VOL. 102, NO. B7, PAGES 14,991–15,019, JULY 10, 1997

Element transport from slab to volcanic front at the Mariana arc

Tim Elliott,[1,2] Terry Plank,[3,4] Alan Zindler,[1,5] William White,[3] and Bernard Bourdon[1,6]

Abstract. We present a comprehensive geochemical data set for the most recent volcanics from the Mariana Islands, which provides new constraints on the timing and nature of fluxes from the subducting slab. The lavas display many features typical of island arc volcanics, with all samples showing large negative niobium anomalies and enrichments in alkaline earth elements and lead (e.g., high Ba/La and Pb/Ce). Importantly, many of these key ratios correlate with a large range in ^{238}U excesses, ($^{238}U/^{230}Th$) = 0.97-1.56. Geochemical features show island to island variations; lavas from Guguan have the largest ^{238}U-excesses, Pb/Ce and Ba/La ratios, while Agrigan lavas have small ^{238}U excesses, the least radiogenic $^{143}Nd/^{144}Nd$, and the largest negative cerium and niobium anomalies. These highly systematic variations enable two discrete slab additions to the subarc mantle to be identified. The geochemical features of the Agrigan lavas are most consistent with a dominant subducted sediment contribution. The added sedimentary component is not identical to bulk subducted sediment and notably shows a marked enrichment of Th relative to Nb. This is most readily explained by melt fractionation of the sediment with residual rutile and transfer of sedimentary material as a melt phase. For most of the highly incompatible elements, the sedimentary contribution dominates the total elemental budgets of the lavas. The characteristics best exemplified by the Guguan lavas are attributed to a slab-derived aqueous fluid phase, and Pb and Sr isotope compositions point toward the subducted, altered oceanic crust as a source of this fluid. Variable addition of the sedimentary component, but near-constant aqueous fluid flux along arc strike, can create the compositional trends observed in the Mariana lavas. High field strength element ratios (Ta/Nb and Zr/Nb) of the sediment poor Guguan lavas are higher than those of most mid-oceanic ridge basalts and suggest a highly depleted subarc mantle prior to any slab additions. The ^{238}U-^{230}Th systematics indicate >350 kyr between sediment and mantle melting but <30 kyr between slab dehydration and eruption of the lavas. This necessitates rapid magma migration rates and suggests that the aqueous fluid itself may trigger major mantle melting.

Introduction

Convergent margin volcanism is a highly tangible consequence of the transfer of material from the subducted slab into the overlying mantle wedge at subduction zones. A flux of water from the descending plate is required to enable mantle melting that results in the formation of volcanic arcs. The compositions of the erupted melts themselves additionally implicate the transport of many other elements from the slab to subarc mantle (see *Gill* [1981] and *Hawkesworth et al.* [1991] for summaries). Specific chemical tracers have been used to identify unambiguously contributions from subducted sediment [*Tera et al.*, 1986; *Monaghan et al.*, 1988; *Morris and Tera*, 1989] and altered oceanic crust [*Ishikawa and Nakamura*, 1994] in arc lavas. Although the chief inputs at subduction zones can thus be finger-printed in the volcanic output, there remain considerable uncertainties as to the nature of processes that transport elements from the slab to subarc mantle and eventually to the surface [*Hawkesworth et al.*, 1993a].

Arc volcanics have highly characteristic incompatible trace element abundance patterns [*Gill*, 1981; *Kay*, 1980; *Saunders et al.*, 1980; *Pearce*, 1982] that provide key, but complex, evidence about the processes of element transport from slab to mantle wedge. Such distinctive chemical signatures have frequently been linked to the flux of water derived from dehydration reactions in the downgoing slab, which is expected to carry a significant budget of elements that are mobile in a water-rich fluid phase [e.g., *Tatsumi et al.*, 1986]. The subarc mantle may thus be enriched in "fluid-mobile" elements such as Rb, K, Ba, and Pb [*Gill*, 1981; *Hawkesworth et al.*, 1991, and references therein]. As is common, we refer collectively to this group of elements as large ion lithophile elements (LILE). Elements that have higher charge density, most notably the high field strength elements (HSFE; Nb, Ta, Zr and Hf) but also Th and rare earth elements (REE), are probably much less readily transported by the fluid phase [*Tatsumi et al.*, 1986; *Brenan et al.*, 1995a,b; *Keppler*, 1996]. The arc

[1]Lamont-Doherty Earth Observatory of Columbia University, Palisades, New York.
[2] Now at Faculteit der Aardwetenschappen, Vrije Universiteit, Amsterdam, Netherlands.
[3]Department of Geological Sciences, Snee Hall, Cornell University, Ithaca, New York.
[4]Now at Department of Geology, 120 Lindley Hall, University of Kansas, Lawrence.
[5]Now at National High Magnetic Field Laboratory and Department of Geology, Florida State University, Tallahassee.
[6]Now at Laboratoire de Géochimie et Cosmochimie, URA-CNRS 1758, Institut de Physique du Globe de Paris, France.

Paper number 97JB00788.
0148-0227/97/97JB-00788$09.00

lava source can thus appear relatively depleted in these "fluid-immobile" elements, resulting most clearly in negative "Nb anomalies." However, some of the geochemical effects of adding an LILE-rich fluid to the subarc mantle can be similar to those of adding pelagic sediment [*White and Patchett*, 1984; *Hole et al.*, 1984; *Ben Othman et al.*, 1989]. For example, many sediments are strongly LILE enriched and have their own, preexisting negative Nb anomalies [*Hole et al.*, 1984; *Vroon et al.*, 1995; T.Plank and C.H.Langmuir, The geochemical composition of subducting sediment and its consequences for the crust and mantle, submitted to Chemical Geology, 1996, hereinafter referred to as Plank and Langmuir, submitted manuscript]. Thus a central issue in modeling arc lavas is deciding how much of the geochemical signal results from subarc transport processes and how much is due simply to the composition of subducted materials.

Many authors have argued for a single subduction component, which fluxes elements from slab to subarc mantle according to their relative aqueous fluid mobility [*Pearce*, 1982; *Tatsumi et al.*, 1986; *McCulloch and Gamble*, 1991]. Aqueous fluid partitioning may not only control the efficiency of element transport from slab to wedge but also may further modify fluid composition during subsequent percolation in the mantle wedge [*Stern et al.*, 1991; *Hawkesworth et al.*, 1993b; *Stolper and Newman*, 1994]. *Kelemen et al.* [1990, 1993], however, have attributed high LILE/HSFE ratios to a melt reaction process that can be modelled with anhydrous mineral-melt partition coefficients, without recourse to aqueous fluid-solid partitioning.

In contrast, *Plank and Langmuir* [1993] stressed the importance of the composition of the subducted sedimentary input in controlling the chemistry of subduction zone volcanics. Lead isotopic studies have also noted a strong coupling between variable signatures of subducted sediment and associated erupted volcanics [*White and Dupré*, 1986; *Woodhead*, 1989, and references therein; *McDermott et al.*, 1993; *Vroon et al.*, 1995]. Nevertheless, some authors have ascribed the radiogenic isotope and some trace element signatures in arc lavas to the presence of enriched mantle (similar to the source of ocean island basalts, OIB) in the mantle wedge, unrelated to the subduction process [*Morris and Hart*, 1983; *Stern and Ito*, 1983; *Reagan and Gill*, 1989; *Stolz et al.*, 1990]. There has also been some debate as to how reliably recycled sediment contributions to the lava source may be distinguished from crustal contamination during shallow level differentiation [*Davidson*, 1987; *Hildreth and Moorbath*, 1988]. Even where the involvement of subducted sedimentary material has been implicated, some studies have further required an independent fluid phase to explain the geochemistry of arc lavas [*Kay*, 1980; *Ellam and Hawkesworth*, 1988; *McDermott et al.*, 1993; *Plank*, 1993; *Miller et al.*, 1994; *Turner et al.*, 1996].

Correctly assessing the relative importance of each of the above processes is crucial in attempting the mass balance of elements at the subduction zone and hence in calculating the flux of continental material recycled into the mantle. In trying to identify subarc processes we examine an arc lava suite using a combination of incompatible element and radiogenic isotope measurements together with ^{238}U-^{230}Th disequilibrium analyses. The ^{238}U-^{230}Th disequilibrium data are particularly powerful as they enable the effects of recent (<350ka) processes, that fractionate U from Th, to be distinguished from older events. In the presence of the oxidizing fluids expected in the subduction zone, U is readily fractionated from Th and thus ^{238}U-^{230}Th disequilibrium should provide a highly sensitive tracer of recent fluid fractionation.

Previous work showed that Mariana arc lavas have a very large range of ^{238}U-^{230}Th disequilibrium [*Newman et al.*, 1984; *Gill and Williams*, 1990; *McDermott and Hawkesworth*, 1991] and so the Marianas appeared to be a suitable location to investigate how disequilibrium varies with other geochemical tracers. Inferences about arc processes have often depended on the particular elements used for investigation. Thus we have assembled an unusually comprehensive set of elemental and isotopic data on a suite of subaerial Mariana arc lavas that gives a multifacetted view of compositional variation. In addition to major element and radiogenic isotope measurements, samples were analyzed for an extensive suite of trace elements by inductively coupled plasma-mass spectrometry (ICP-MS), which notably provides high-precision concentration data for HSFE as well as other elements that are typically underrepresented in many studies (e.g., Pb, Cs).

Geological Setting and Sample Selection

The intraoceanic Mariana arc is comparatively simple in its tectonic setting. It forms part of the 2500 km long Izu-Bonin-Mariana (IBM) arc system, resulting from westward subduction of the Pacific Plate beneath the Philippine Sea Plate (Figure 1). Jurassic Pacific crust is subducted beneath the Marianas at a convergence rate of ~4 cm/yr [*Seno*, 1977]. The IBM arc has been active since 45 Ma [*Meijer et al.*, 1983] and has been associated with major backarc spreading, which is currently manifest in the 7 Ma Mariana Trough [*Fryer and Hussong*, 1981]. Backarc spreading has further isolated the present arc system from terrigenous continental input. *Bloomer et al.* [1989] divided the Mariana section of the IBM arc into three provinces; Southern Seamount, Central Island, and Northern Seamount. The samples in this study (Table 1) come from seven of the nine, modest sized (2-45 km^2) islands (Figure 1), which form part of the Central Island province. These islands have experienced abundant, dominantly mafic, historic, and Holocene eruptions [*Meijer*, 1982].

Except for three samples (prefixed MM in Table 1) kindly provided by R. B. Moore of the U. S. Geological Survey, all samples were specifically collected for U series isotopic analysis by T. E.. Disequilibrium between ^{238}U and ^{230}Th persists only ~350 kyr, and so samples must be younger than this, preferably less than 10 kyr so that no age corrections (with attendant additional errors) need be made. Some samples (Table 1) were taken from flows that clearly correspond to the 14 historic eruptions reported for the Mariana islands [*Simkin et al.*, 1981]. Other samples are not so irrefutably young but were taken from flows with fresh flow tops or only minor additional coverage of ash or later flows. The samples thus represent the very youngest available material on the islands. Detailed mapping, combined with ^{14}C analyses, indicate that most of the exposed portions of the islands investigated are younger than 10 ka (R. B. Moore, personal communication, 1992). Hence we are confident that all samples in this study are suitably young to require no age corrections for ^{238}U-^{230}Th disequilibrium measurements.

In addition to being tectonically simple and a favorable location for studying ^{238}U-^{230}Th disequilibrium, the Mariana arc also has the advantage that its sedimentary input can be assessed comparatively well. There is no evidence of sediment accumulation in an accretionary prism [*von Heune and Scholl*,

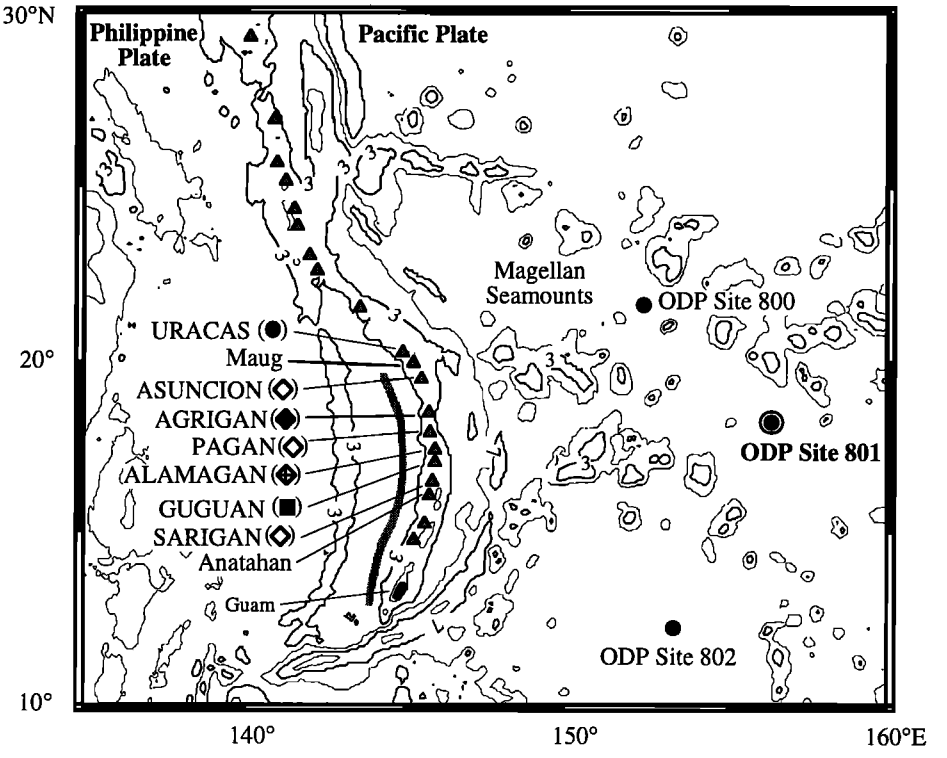

Figure 1. Map of the Mariana arc. The nine islands of the Central Island province of the Mariana arc are labeled. Those islands that form part of this study are shown in capitals, together with their respective symbols used in subsequent plots. Other major volcanic edifices of the Mariana arc, from the Northern and Southern Seamount provinces (respectively to the north and south of the islands) are shown as unmarked, solid triangles. Guam, part of an earlier phase of arc volcanism, is also labeled as a reference point. The grey line behind the volcanic front marks the current axis of backarc rifting. Ocean Drilling Program (ODP) Leg 129 drill sites are shown as solid dots. Hole 801 of ODP Leg 129, used in calculation of bulk Mariana sediment composition, is shown in bold. Contours are marked in kilometers below sealevel.

1991; *Taylor*, 1992], and so the entire sediment pile is subducted. Furthermore, the composition of the sedimentary column on the subducting Pacific Plate is well constrained from three deep drill holes of Ocean Drilling Program (ODP) Leg 129 [*Lancelot et al.*, 1990] (Figure 1).

To estimate the chemistry of bulk subducted sediment, we have used samples from Hole 801 of ODP Leg 129, which penetrated the complete sedimentary cover. The stratigraphy of Hole 801 comprises an upper 65 m layer of Cenozoic brown clay, underlain by 60 m of Upper Cretaceous chert, 190 m of Albian volcaniclastic turbidites of OIB affinity and 140 m of largely Jurassic radiolarite [*Lancelot et al.*, 1990]. There are both downhole geochemical logs [*Pratson et al.*, 1992] and a large number of existing major and trace element analyses of samples from throughout the core [*Karl et al.*, 1992; *Karpoff*, 1992]. The budgets of most incompatible elements considered in this study are dominated by the pelagic clay and volcaniclastics, and so representative samples from these units were the focus of further analysis by ICP-MS. The bulk composition of the sediment column (Table 2) was estimated using the methodology of *Plank and Ludden* [1992].

There is broad agreement between many features of our sediment estimate and the bulk western Pacific sediment of *Lin* [1992]. However, some of the elemental abundances (e.g., Th and Nb) important to this study were not analyzed by *Lin* [1992], and close correspondence of the two bulk sediment estimates is not necessarily expected. *Lin* [1992] constructed a western Pacific composite with 10 lithologically averaged, but geographically widely spaced samples. We focused solely on the Mariana arc, using samples from a single core directly off-board the arc. Eleven individual ICP-MS analyses could then be weighted using the abundant additional major element and lithological constraints for this core (Plank and Langmuir, submitted manuscript, 1996). *Hole et al.* [1984] also calculated a bulk sediment composition (PAWMS) for their discussion of the petrogenesis of the Mariana volcanics but used analyses of rather different sediment compositions from the other side of the Pacific.

Results

There have been numerous previous trace element and isotopic investigations of the subaerial Mariana volcanics [*Meijer*, 1976; *Dixon and Batiza*, 1979; *Stern*, 1979; *Chow et al.*, 1980; *Meijer and Reagan*, 1981; *Stern and Ito*, 1983; *Hole et al.*, 1984; *White and Patchett*, 1984; *Ito and Stern*, 1985/1986; *Woodhead and Fraser*, 1985; *Woodhead et al.*, 1987; *Woodhead*, 1989], and not surprisingly, the samples from this study show many of the features already reported in the literature. Thus this section only briefly summarizes the general characteristics of the lavas and then focuses on some new features revealed by our data.

The volcanics analyzed are generally basalts and basaltic andesites (Figure 2a). Most lavas are phyric, and phenocrysts

include olivine, plagioclase, clinopyroxene, and titanomagnetite. Fractionation of these phases appears to play an important role in controlling major element variations within the Mariana Island lavas [*Dixon and Batiza*, 1979; *Stern*, 1979; *Meijer and Reagan*, 1981; *Woodhead*, 1988], although there is also much petrological evidence for mixing and crystal accumulation/stagnation (particularly of plagioclase). The lavas do not fall on a single liquid line of descent (Figure 2a), and even analyses of tephra glasses derived from the Mariana arc show multiple differentiation paths [*Lee et al.*, 1995]. Thus it is difficult to reliably correct for crystal fractionation, and so we characterize lavas using highly incompatible element ratios that should remain largely unaffected by crystal fractionation/accumulation (and are also generally little fractionated by mantle melting). Throughout this paper we refer to "highly incompatible" elements as those inferred to be more incompatible than Ce during mantle melting (i.e., those elements to the left of Ce in Figure 3).

The lavas of this study show a large range of highly incompatible element contents; Th contents vary by a factor 6,

Table 1. Analyses of Lavas from the Mariana Islands

	Sample									
	SAG 1	GUG 3	GUG 4	GUG 6	GUG 9	GUG 11	GUG 12	GUG 13	ALAM 2	ALAM 5
Latitude N	16° 42.4'	17° 19.1'	17° 19.1'	17° 19.6'	17° 19.8'	17° 19.9'	17° 20.0'	17° 19.2'	17° 37.0'	17° 35.2'
Longitude E	145° 48.7'	145° 50.4'	145° 50.4'	145° 50.7'	145° 50.8'	145° 50.9'	145° 50.9'	145° 50.3'	145° 49.6'	145° 49.7'
Eruption date				1883 (?)	1883					
SiO_2	53.37	51.61	52.37	51.14	50.99	52.96	52.16	51.78	54.95	53.39
TiO_2	0.78	0.86	0.82	0.82	0.82	0.81	0.81	0.81	0.78	0.81
Al_2O_3	16.23	19.75	17.54	19.85	19.60	19.88	20.04	19.94	17.40	17.17
Fe_2O_3T	9.83	9.93	10.26	10.00	10.07	9 32	9.73	9.67	9.58	10.05
MnO	0.19	0.19	0.20	0.18	0.18	0.18	0.18	0 18	0.18	0.19
MgO	5.57	3.36	5.22	3.99	4.23	3.38	3.49	3.47	4.40	4 86
CaO	10.45	10.50	10.41	11.07	11.05	10.22	10.73	10.66	8.98	9.97
Na_2O	2.71	2.69	2.64	2.62	2.56	2.95	2 67	2.55	2 98	2.70
K_2O	0.72	0.91	0.55	0.43	0.43	0.51	0.45	0.44	0.94	0.83
P_2O_5	0.13	0.17	0.10	0.09	0.09	0 10	0.09	0.09	0.14	0.14
Total	99.96	99.97	100.11	100.18	100.00	100.29	100.36	99.58	100.36	100.13
Zn	78	82	86	74	81	78	79	78	79	82
Ni	29	13	24	20	15	15	29	12	20	18
Cr	63	5	37	10	12	4	53	2	20	22
V	233	279	259	283	227	241	286	265	218	264
Rb	9.5	16 9	8.1	6.3	6.5	7.2	7.4	6.1	16.3	15 4
Cs	0.353	0.467		0.330		0 271	0.198			0 589
Sr	352	401	291	309	299	306	281	303	303	307
Ba	253	217	167	160	139	190	172	162	251	238
La	6.17	7.40	3.55	3.14	2.85	3.18	3.26	2.75	5.90	5.85
Ce	13.98	15 86	9.11	8.23	7.63	8.53	8.43	7.53	14.04	13.51
Pr	2.14	2.40	1.50	1 38	1.30	1 46	1.40	1.28	2.17	2 12
Nd	10.01	11.11	7.58	7.02	6.57	7.47	7.08	6.59	10 33	10.12
Sm	2.86	3.08	2 39	2.25	2 14	2.43	2.27	2.21	3.05	2.99
Eu	1.01	1.08	0.86	0.85	0 81	0.92	0.84	0.83	0.97	1.01
Gd	3.51	3.65	3.23	2.91	2.86	3.19	2.94	2.96	3.86	3 73
Tb	0.644	0.657	0.600	0.562	0.547	0.626	0 559	0.573	0.727	0.693
Dy	3.75	3.81	3.57	3.38	3.29	3 72	3.38	3.51	4.29	4.10
Ho	0 787	0.816	0.791	0.743	0.727	0.830	0 743	0.781	0.933	0.890
Er	2.29	2.30	2 26	2.13	2.11	2.38	2.15	2 17	2 69	2.54
Tm	0.362	0.358	0.359	0.338	0.326	0.377	0.339	0.353	0.431	0.401
Yb	2.28	2.29	2 30	2.18	2.07	2.46	2.18	2.22	2.73	2.53
Lu	0.350	0.356	0.365	0.345	0.331	0.391	0.345	0.358	0.443	0.394
Y	23.5	23.0	22.8	20.9	20.1	23.5	21.7	21.6	26.7	24 1
Hf	1.90	1.78	1.63	1 52	1.42	1.70	1 50	1.55	2.33	2.18
Ta	0 120	0.092	0.070	0.073	0.061	0.069	0 066	0.059	0.093	0.095
Zr	68.5	66.3	57.9	53.0	50.4	60.0	53.5	53.4	82.9	74.4
Nb	1.64	1.24	0.81	0.78	0.73	0.70	0 72	0.67	1 30	1.24
Th	0.828	0.737	0.367	0.276	0 266	0 282	0.319	0 252	0.799	0.770
U	0.362	0.358	0.198	0.154	0.150	0.180	0.202	0.155	0 423	0.380
Pb	3.63	2.82	2.42	0.86	2.03	2.44	1 81	1.92	3.14	3 24
$(^{230}Th/^{232}Th)$	1.141	1.145	1.221	1.228	1.212	1.269	1.234	1.233	1.418	1.346
$(^{238}U/^{230}Th)$	1.164	1.286	1.339	1.374	1.412	1.525	1.560	1.512	1.133	1.112
$^{87}Sr/^{86}Sr$	0.70343	0.70348	0.70347		0.70345	0.70350		0.70349	0.70356	0.70365
$^{143}Nd/^{144}Nd$	0.512959	0.512945	0.513038	0.513042	.513043	0.513052	0.513037	0.513043	0.513006	0.513017
$^{206}Pb/^{204}Pb$	18.986	18.847						18.781		
$^{207}Pb/^{204}Pb$	15.633	15.597						15.575		
$^{208}Pb/^{204}Pb$	38.612	38.505						38.413		

while Nb and Ba vary threefold (Figures 2b and 2c). For the data set as a whole, incompatible element ratios vary as their concentrations increase (Figures 2b and 2c). Such incompatible element variations cannot be related to crystal fractionation alone (Fig. 2b and 2c); see also *Meijer and Reagan* [1983]. However, for lava suites from individual islands, variations of incompatible element concentrations occur without a change in their ratios and can be reasonably explained as a result of differentiation (Figures 2b and 2c). Since we are mostly interested in geochemical variations related to deep processes, it is interisland differences in lava composition that are most important.

Guguan lavas have much lower Th and Nb contents than those from Agrigan or Uracas (Figure 2b), greater than can be related to any differences in degrees of differentiation, and also significantly different Th/Nb and Ba/Nb ratios (Figures 2b and 2c). The distinction between Guguan and Agrigan (or Uracas) lavas is evident in many subsequent plots (as is the systematic departure of the single sample GUG3 from the main body of Guguan analyses). Compositions of the Central Island

Table 1. (continued)

	Sample									
	PAG1	PAG2	PAG3	MM-92-10	AGR1	AGR2	AGR 4b	AGR 5	AGR 8b	MM-92-6
Latitude N	18° 09.4'	18° 09.4'	18° 09.5'	18° 07.4'	18° 43.9'	18° 44.4'	18° 48.0'	18° 47.4'	18° 43.9'	18° 46 4'
Longitude E	145° 47.8'	145° 47.8'	145° 47.2'	145° 45.8'	145° 39.2'	145° 38.9'	145° 38.9'	145° 38.4'	145° 40.3'	145° 40.0'
Eruption date	1923 (?)	1923 (?)	1981							1917
SiO_2	51.34	49.83	51.64	54.46	51.58	50.94	50.48	51.29	50.50	55.24
TiO_2	0.91	0.70	0.93	1.22	0.75	0.79	0.76	0.64	0.73	0.87
Al_2O_3	15.87	17.59	15.73	15.13	20.19	16.84	18.45	17.74	20.20	16.49
Fe_2O_3T	12.19	10.48	12.23	12.39	9.77	12.45	11.08	10.43	9.83	10.67
MnO	0.22	0.19	0.22	0.24	0.19	0.23	0.21	0.20	0.19	0.24
MgO	5.45	6.20	5.25	3.23	3.04	4.98	4.80	5.38	3.55	3.15
CaO	10.60	12.07	10.25	7.44	10.71	10.46	10.83	10.89	11.15	7.68
Na_2O	2.80	2.24	2.72	3.44	2.72	2.85	2.60	2.55	2.58	3.56
K_2O	0.75	0.56	0.78	1.45	1.03	0.74	0.85	0.86	0.89	1.41
P_2O_5	0.14	0.10	0.15	0.29	0.19	0.15	0.17	0.14	0.17	0.27
Total	100.28	99.94	99.88	99.28	100.18	100.45	100 23	100.11	99.78	99.59
Zn	99	76	100	140	76	90	79	81	76	116
Ni	23	47	26	5	10	12	16	15	12	11
Cr	36	103	45		5	6	6	12	6	
V	365	291	373	289.4	246	341	262	243	257	205
Rb	11.9	8.7	12.5	24.1	22.5	13.0	18.0	16.7	19.9	31.5
Cs						0.160	0.171	0.289	0.463	0.733
Sr	334	348	317	321	394	344	377	318	395	324
Ba	221	175	230	404	181	158	177	183	165	278
La		3.80	5.18	10.55		6.84	7.56	7.49	7.45	11.41
Ce		9.11	12.45	23.90		14.71	16.02	15.97	15.76	23.98
Pr		1.44	1.95	3.82		2.24	2.41	2.40	2.34	3.53
Nd		7.04	9.57	17.44		10.48	11.08	10.95	10.73	15.88
Sm		2.18	2.95	4.95		2.90	2.95	2.84	2.79	4.11
Eu		0.78	1.01	1.58		1.03	1.04	0.93	0.99	1.37
Gd		2.71	3.69	5.91		3.33	3.27	3.20	3.17	4.84
Tb		0.482	0.670	1.055		0.603	0.586	0.592	0.563	0.874
Dy		2.89	3.93	6.24		3.47	3.30	3.30	3.16	4.93
Ho		0.630	0.853	1.343		0.741	0.698	0.708	0.667	1.058
Er		1.74	2.40	3.78		2.09	1.95	2.04	1.87	2.98
Tm		0.274	0.370	0.599		0.321	0.307	0.318	0.291	0.470
Yb		1.74	2.36	3.73		2.01	1.90	1.99	1.86	2.94
Lu		0.277	0.369	0.585		0.316	0.297	0.319	0.288	0.472
Y		17.1	23.2	37.2		20.1	19.5	20.0	18.1	29.8
Hf		1.19	1.80	3.26		1.52	1.61	1.85	1.60	2.59
Ta		0.049	0.071	0.139		0.065	0.073	0.080	0.088	0.117
Zr		41.8	60.8	116.6		51.9	58.9	64 5	59.2	96.3
Nb		0.69	0.96	2.17		1.01	1.15	1.23	1.13	1.86
Th	0.526	0.389	0.547	1.160	1.020	0.813	0 838	0.944	0.881	1 376
U	0.267	0.196	0.287	0.583	0.424	0.311	0.354	0.386	0.383	0.578
Pb		2.01	2.71	4.70		1.83	1.20	2.03	1.79	3.01
$(^{230}Th/^{232}Th)$	1.187	1.164	1.192	1 227	1.119	1.097	1.122		1.126	1.135
$(^{238}U/^{230}Th)$	1.298	1.312	1.337	1.242	1.126	1.057	1.141		1.171	1.124
$^{87}Sr/^{86}Sr$	0.70350	0.70350	0.70353		0.70336	0.70337	0.70338			
$^{143}Nd/^{144}Nd$	0.513005	0.513011	0.513011	0.513009	0.512990	0.512992	0.512981	0.512996	0.512987	0 512987
$^{206}Pb/^{204}Pb$	18.856	18.839		18.849	18.787	18.757	18.810			18.788
$^{207}Pb/^{204}Pb$	15.616	15.569		15.605	15.566	15.553	15.583			15.567
$^{208}Pb/^{204}Pb$	38.578	38.427		38.548	38.423	38.372	38.472			38.431

Table 1. (continued)

	Sample								
	ACS 3	URA 5	URA 6	URA 7	URA 12	BHVO-1	S.D., %	JA-1	S.D., %
Latitude N	19° 42.0'	20° 32.4'	20° 32.4'	20° 32.4'	20° 32.7'				
Longitude E	145° 23.8'	145° 51.9'	145° 51.9'	145° 51.8'	145° 51.3'				
Eruption date	1906	1900-52	1900-52	1900-52					
SiO_2	54.49	53.57	59.92	54.17	53.77	49.72	0.06		
TiO_2	0.87	0.63	0.83	0.77	0.75	2.79	0.14		
Al_2O_3	17.92	16.63	15.39	19.20	19.62	13.65	0.09		
Fe_2O_{3T}	9.97	9.61	9.99	9.73	9.55	12.03	0.10		
MnO	0.19	0.18	0.23	0.19	0.19	0.17	0.47		
MgO	3.27	6.13	2.25	2.71	2.68	6.68	0.28		
CaO	9.44	10.52	6.20	9.64	9.93	11.36	0.09		
Na_2O	3.01	2.29	3.85	2.88	2.81	2.38	0.95		
K_2O	0.60	0.53	1.10	0.76	0.70	0.54	0.21		
P_2O_5	0.13	0.09	0.19	0.13	0.13	0.28	0.91		
Total	99.89	100.20	99.95	100.19	100.13	99.61			
Zn	88	72	111	86	83	108	0.8		
Ni	15	26	5	11	9	156	12		
Cr	4	49	0	2	2	285	28		
V	232	235	120	232	208	284	0.8		
Rb	9.6	8.2	18.3	12.0	11.9	8.9	4.2	11.8	2.9
Cs		0.365	0.675					0.670	0.6
Sr	286	307	319	384	398	389	0.5	263	3.0
Ba	188	198	424	290	245	132	3.2	312	5.0
La	4.77	4.45	10.05	7.97	7.29			4.96	9.1
Ce	11.74	10.17	22.20	16.80	15.57			13.42	4.1
Pr	1.91	1.54	3.19	2.41	2.21			2.24	4.2
Nd	9.30	7.25	14.92	10.75	9.98			11.23	4.8
Sm	2.93	2.15	4.30	2.97	2.79			3.52	7.2
Eu	1.04	0.81	1.45	1.07	1.00			1.17	4.7
Gd	3.71	2.80	5.33	3.68	3.41			4.48	1 9
Tb	0.717	0.528	1.014	0.699	0.638			0.849	2.8
Dy	4.29	3.19	6.04	4.19	3.80			5.04	2.3
Ho	0.916	0.696	1.345	0.882	0.827			1.097	2.7
Er	2.66	1.99	3.85	2.56	2.34			3.11	2.7
Tm	0.428	0.320	0.610	0.406	0.374			0.490	2.9
Yb	2.70	2.05	3.92	2.55	2.35			3.08	3.6
Lu	0.432	0.324	0.617	0.406	0.385			0.491	2.6
Y	26.0	20.2	36.4	24.0	23.0	24 6	1.1	29.9	2.7
Hf	1.77	1.37	2.78	1.76	1.66			2.70	3.8
Ta	0.067	0.072	0.143	0.101	0.092			0.110	7.9
Zr	63 0	49.0	96.1	62.6	59.4	177.3	0.9	88.8	4.0
Nb	0.95	1.04	2.11	1.66	1.60	19	19	1.30	0.8
Th	0.514	0.597	1.406	1.224	1.132			0.774	4 5
U	0.224	0.238	0.511	0.407	0.377			0.353	1.9
Pb	2.10	2.06	4.23	2.76	2.59			5.84	4.3
$(^{230}Th/^{232}Th)$	1.140	1.126	1.097	1.040	1.044				
$(^{238}U/^{230}Th)$	1.162	1.074	1.005	0.970	0.967				
$^{87}Sr/^{86}Sr$	0.70344	0.70365	0.70359	0.70354	0.70354				
$^{143}Nd/^{144}Nd$	0.513033	0.513010	0.512990	0.512984	0.512966				
$^{206}Pb/^{204}Pb$	18.762	18.950	18.881		18.860				
$^{207}Pb/^{204}Pb$	15.573	15.638	15.602		15.575				
$^{208}Pb/^{204}Pb$	38.451	38.793	38.587		38.517				

Samples collected specifically for this study are labeled with an abbreviation of the island name and those from a U. S. Geological Survey expedition, kindly provided by R. M. Moore, are prefixed MM-92 (MM-92-10 comes from Pagan and MM-92-6 comes from Agrigan). Major elements were measured by XRF and reported in weight percent, and trace elements were measured by a combination of XRF (Zn, Ni, Cr, V, Rb, Sr and Ba) and ICP-MS (other trace elements except Th and U, where isotope dilution measurements are cited) and are reported in parts per million by weight. Isotopic ratios are atomic ratios except for ^{238}U series measurements which are reported as activity ratios. Blank spaces imply no analysis made. Where elements were analyzed by several techniques, only one set of data is quoted. Values obtained for BHVO-1 and JA-1, analyzed as unknowns during XRF and ICP-MS measurements respectively are shown together with 1 sigma standard deviations expressed as percents of the measured value. BHVO-1 was measured eight times and JA-1 in triplicate. The reproducibilities cited for JA-1 are maxima as these measurements were made over a period of machine development of the ICP-MS. For some elements, the reproducibility of BHVO-1 is not a good guide to sample reproducibility, and in these cases (Ni, Cr and Nb) an average of percent standard deviation between duplicate analyses (made for all samples) is quoted in preference. Ages are attributed to samples where there are obvious recent flows that correspond to documented historic eruptions [*Simkin et al.*, 1981]. Uracas has experienced much recent activity, and the recent flows cannot be related to a specific date but simply to the abundant eruptions between 1900 and 1952.

Table 2. Estimates of the Composition of the Chief Sedimentary Units and Bulk Sediment Column Drilled by Hole 801 ODP Leg 129

Unit	Brown Clay	Brown Chert	Volcaniclastic Turbidites	Brown Radiolarite	Bulk Sediment
Thickness, m	65	60	190	140	455
Density, g/cm^3	1.4	1.8	1.8	2.1	1.8
Water, wt %	55.4	12.5	28.9	12.4	23.9
SiO_2	51.40	83.56	69.20	89.44	78.67
TiO_2	0.61	0.41	1.27	0.13	0.63
Al_2O_3	15.40	3.56	6.22	1.89	4.59
FeO_T	7.23	2.51	6.37	2.75	4.33
MnO	1.70	0.22	0.11	0.02	0.19
MgO	3.13	0.86	5.31	0.47	2.49
CaO	2.31	0.30	2.87	0.09	1.30
Na_2O	3.64	0.81	1.80	0.26	1.13
K_2O	3.93	0.77	1.62	0.61	1.21
P_2O_5	1.01	0.09	0.24	0.04	0.18
Sum	89.64	92.45	93.34	92.77	92.74
L.O.I.	9.63	7.29	5.91	6.79	6.71
Zn	159	35	81	34	60
Ni	313	19	141	26	87
Cr	53	11	321	13	134
Rb	93	17	24	34	31
Cs	6.6	0.7	0.3	2.0	1.4
Sr	196	76	249	49	140
Ba	319	125	125	889	442
La	104	12	19	8	19
Ce	136	13	36	12	29
Pr	29.9	2.6	4.9	2.4	5.1
Nd	123.00	11	20	9.0	21
Sm	27.0	2.7	4.1	1.9	4.4
Eu	6.3	0.6	1.2	0.5	1.1
Gd	29.2	2.3	3.7	1.9	4.4
Tb	4.90	0.40	0 61	0.32	0.73
Dy	27.1	2.3	3.0	1.8	3.9
Er	14.8	1.4	1.4	1.0	2.1
Yb	13.0	1.2	1.2	1.0	1.9
Lu	2.00	0.18	0.17	0.16	0.28
Y	192.0	10.4	14.3	6.8	22.0
Hf	4.2	1.4	3.8	1.2	2.4
Ta	0.81	0.41	1.66	0.29	0.87
Zr	163	85	144	50	99
Nb	13.1	6.7	23.7	4.0	12.6
Th	9.6	2.0	2.4	1.9	2.6
U	2.0	0.3	0.4	0.4	0.5
Pb	46.4	4.2	2.6	5.1	6.6
Ce/Ce*	0.60	0.57	0.92	0.67	0.72
$^{87}Sr/^{86}Sr$	0.7082	0.7106	0.7045	0 7106	0.7062
$^{143}Nd/^{144}Nd$	0.5124	0.5124	0.5128	0.5124	0.5125
$^{206}Pb/^{204}Pb$	18.69	18.85	19.76	18.85	18.92
$^{207}Pb/^{204}Pb$	15.62	15.68	15.64	15.68	15.65
$^{208}Pb/^{204}Pb$	38.71	38.96	39.44	38.96	38.92

These averaged compositions are calculated using the technique of *Plank and Ludden* [1992] and data from *Karl et al.* [1992] and *Karpoff* [1992] together with ICP-MS analyses on key samples, 11 in total (Plank and Langmuir, submitted manuscript, 1996). Concentrations are expressed as percent (major elements) and parts per million (trace elements) by weight relative to dry sediment mass. Isotopic ratios are derived using data taken from several sources [*Meijer*, 1976; *Woodhead and Fraser*, 1985; *Woodhead*, 1989; *Lin*, 1992].

province as a whole are generally bracketed by the lavas from Guguan and Agrigan (or Uracas).

A more complete range of incompatible element abundances is shown in Figure 3 for samples from Guguan and Agrigan with similar silica contents. The bulk Mariana sediment composition is also shown. The logarithmic scale hides much of the detail of interisland variation evident on subsequent linear trace element plots, but the figure does give a useful overview of some of the distinctive trace element features of the Mariana island lavas. For example, both Guguan and Agrigan lavas have negative Nb anomalies (e.g., high Th/Nb), general enrichments of the highly incompatible elements and pronounced positive lead and strontium concentration "spikes." These features are typical of island arc basalts in general (e.g., the compilation of *McCulloch and Gamble* [1991]). Some major differences between Guguan and Agrigan lavas are also

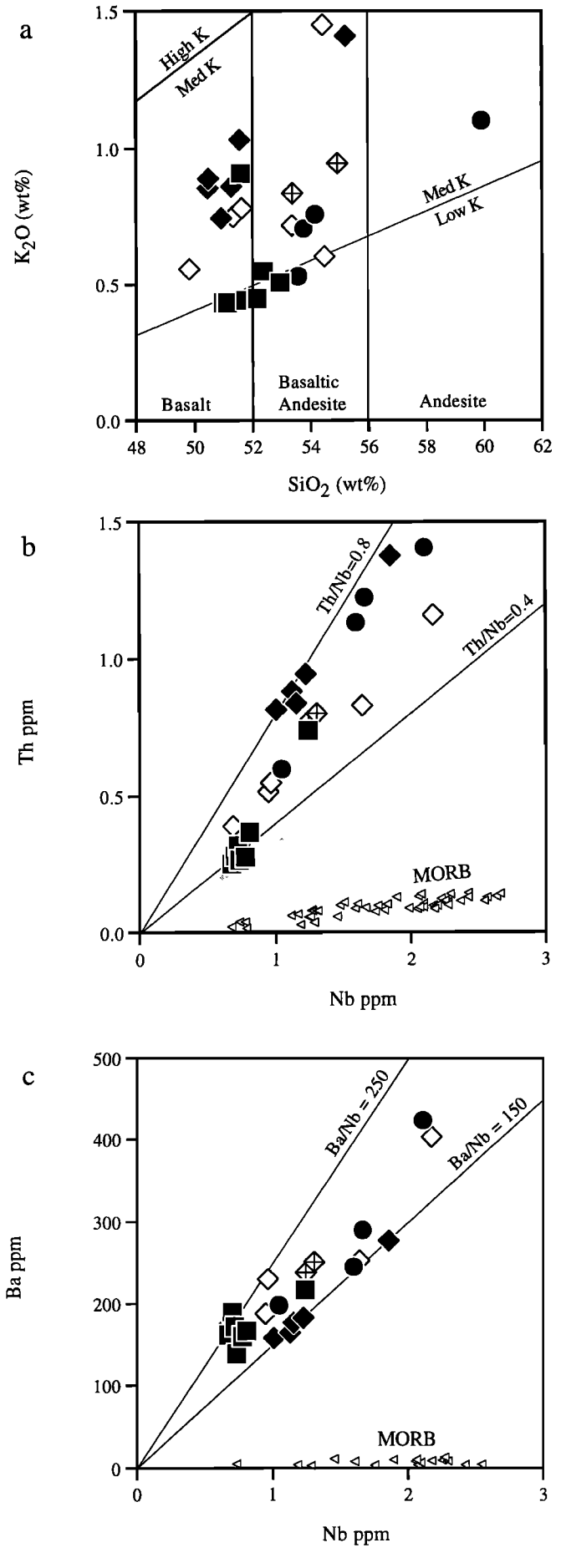

clear in Figure 3. The Agrigan lavas have greater concentrations of most highly incompatible elements (at a given degree of differentiation) and higher light/heavy REE ratios than the Guguan lavas. We thus term the Agrigan and Guguan lavas as "enriched" and "depleted," respectively.

The ^{238}U-^{230}Th disequilibrium data for the lavas of this study are plotted on an equiline diagram in Figure 4a and are compared to MORB, OIB, and other arc data in Figure 4b. The new Mariana ^{238}U-^{230}Th data are compatible with data from earlier studies [*Newman et al.*, 1984; *Gill and Williams*, 1990; *McDermott and Hawkesworth*, 1991]. However, the larger number of analyses undertaken here, together with the higher precision of the mass spectrometric measurements, enables additional detail to be resolved. There is a large range of disequilibrium, from minor ^{230}Th excesses ($^{238}U/^{230}Th$)=0.97 to large ^{238}U excesses ($^{238}U/^{230}Th$)=1.56. In keeping with common usage, ratios in parentheses are activity ratios. The sample array in Figure 4a is slightly inclined, so that lavas with the greatest ^{238}U excesses and U/Th also have the highest ($^{230}Th/^{232}Th$), although the total range in ($^{230}Th/^{232}Th$) is rather small. The Mariana lavas have a large range of U/Th, but even the lowest U/Th ratios are as high as in many MORB (Figure 4b).

The Alamagan samples do not plot on the array defined by the other lavas in Figure 4a and show significantly higher ($^{230}Th/^{232}Th$). However, Alamagan lavas are not distinctive in terms of any other geochemical parameters (Figures 2-11); for example, their ($^{238}U/^{232}Th$) and Th/Nb ratios lie in the middle of the range displayed by sample set as a whole (Figures 2b and 4a). Hence we suggest that the high ($^{230}Th/^{232}Th$) of Alamagan lavas are not due to their being radically different compositions but simply a result of ingrowth of ^{230}Th from the decay of ^{238}U excesses. The Alamagan lava flows themselves are clearly very young, and have ^{40}Ar-^{39}Ar ages younger than 25 ka (M. Pringle, personal communication, 1996]. Thus, we argue that the ^{230}Th ingrowth is not the result of aging on the surface but reflects a longer (~100 kyr) period between production of disequilibrium and eruption at Alamagan compared to the other islands.

The large variations in ^{238}U-^{230}Th disequilibrium in the Mariana lavas notably correlate with incompatible element ratios (Figure 5). ^{238}U excesses vary inversely with Th/Nb (Figure 5a) but positively with Ba/Nb (Figure 5b). Large ^{238}U

Figure 2. (opposite) (a) SiO_2 versus K_2O (weight percent), (b) Nb versus Th concentrations (μg/g), and (c) Nb versus Ba (μg/g) for the Mariana volcanics of this study: Guguan, solid squares; Agrigan, solid diamonds; Uracas, solid circles; Alamagan, crossed open diamonds; other islands, open diamonds. Fields for petrologic classification in Figure 2a are after *Peccerillo and Taylor* [1976] and *Gill* [1981]. Arrows in Figures 2b and 2c indicate the maximum effects of crystal fractionation. The calculation assumes the elements are perfectly incompatible and 50% fractional crystallization, taken from estimates of *Dixon and Batiza* [1979] and *Woodhead* [1988] to explain major element compositional spans equivalent to the total range observed in the lavas of this study. Mid-ocean ridges basalt (MORB) data [*Jochum et al.*, 1983; *Hofmann et al.*, 1986; *Dosso et al.*, 1993] are shown in Figure 2b as left pointing open triangles. The scales in Figures 2b and 2c are restricted so as not to unduly compress the Mariana data and results in some MORB samples with higher Nb concentrations (and all OIB data) being off-scale.

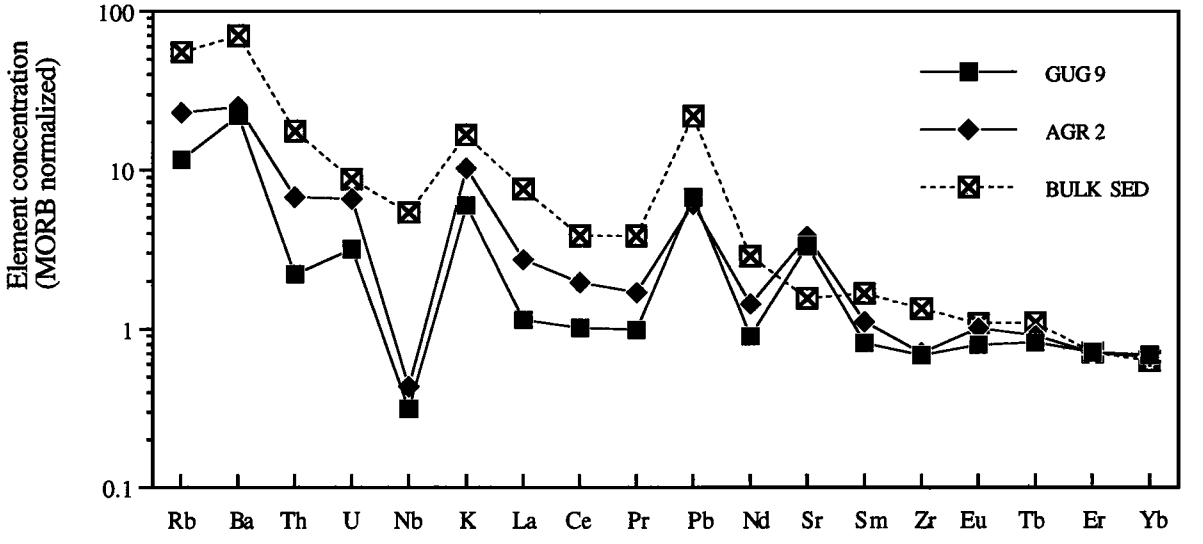

Figure 3. Incompatible element compositions of end-member volcanics of this study, Guguan (GUG 9, solid squares) and Agrigan (AGR 2, solid diamonds), and Hole 801 bulk sediment (crossed open squares). GUG 9 (51.0% SiO_2) and AGR 2 (50.9% SiO_2) appear to have experienced similar degrees of differentiation and are some of the less evolved lavas of the study. Hence comparisons of absolute elemental abundances, particularly of the highly incompatible elements, have some significance. Element concentrations are reported relative to an average normal (N) MORB composition [*Sun and McDonough*, 1989]. The elements are plotted along the abscissa, from left to right, in decreasing order of incompatibility during melting beneath mid-ocean ridges as inferred by *Hofmann* [1988].

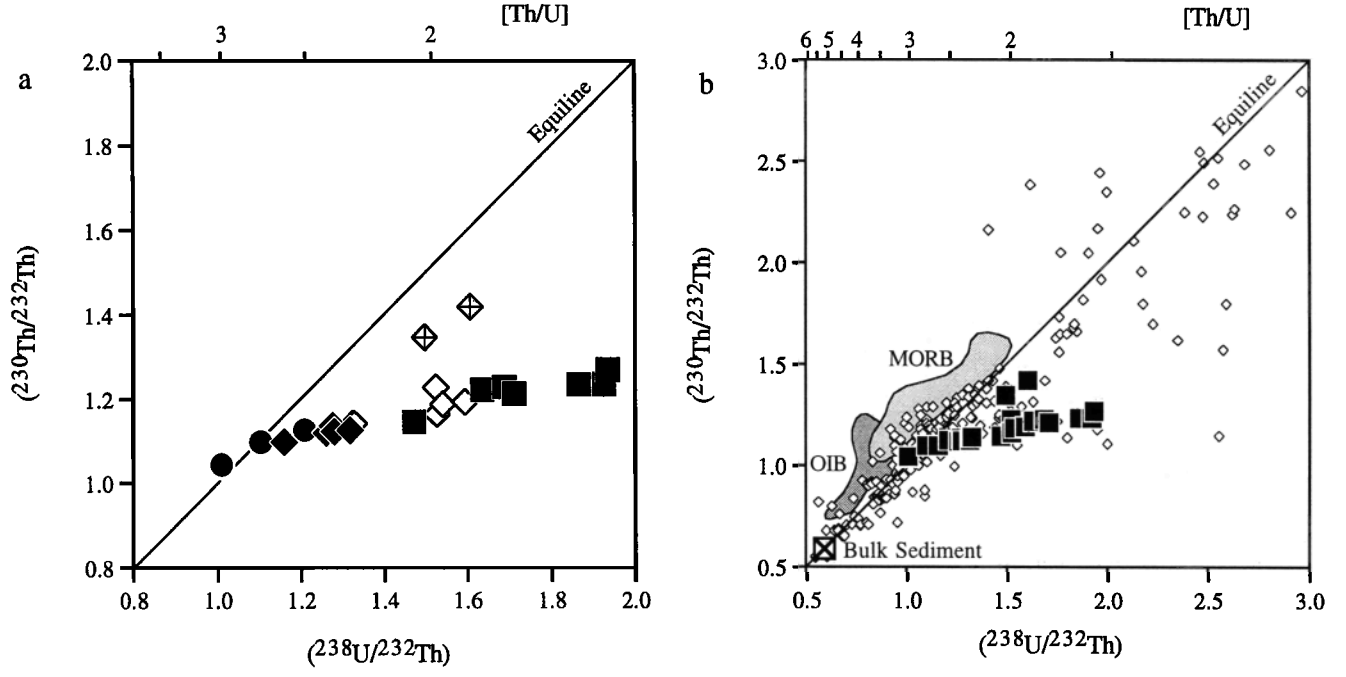

Figure 4. (a) Equiline plot of Mariana lavas from this study (symbols as in Figure 2). Reproducibility (2 σ) is smaller than symbol size. (b) Comparison of ^{238}U-^{230}Th disequilibrium measurements of this study (solid squares) with literature data for other arcs (open diamonds), MORB (light grey field), and OIB (dark grey field). The bulk sediment estimate from this study (crossed square) is plotted assuming it is in secular equilibrium. The very large range of $(^{238}U/^{232}Th)$ and $(^{230}Th/^{232}Th)$ in island arc lavas is evident, but as a consequence, the scale rather compresses additional detail. It is thus not readily apparent that the majority of arc lavas plot close to the equiline [*McDermott and Hawkesworth*, 1991; *Condomines and Sigmarsson*, 1993], although the figure does illustrate that large ^{238}U excesses in basaltic magmas are unique to the arc environment. In both Figures 4a and 4b, Th/U weight ratios are marked along the top of graph for comparison with the perhaps less familiar $(^{238}U/^{232}Th)$ ratios.

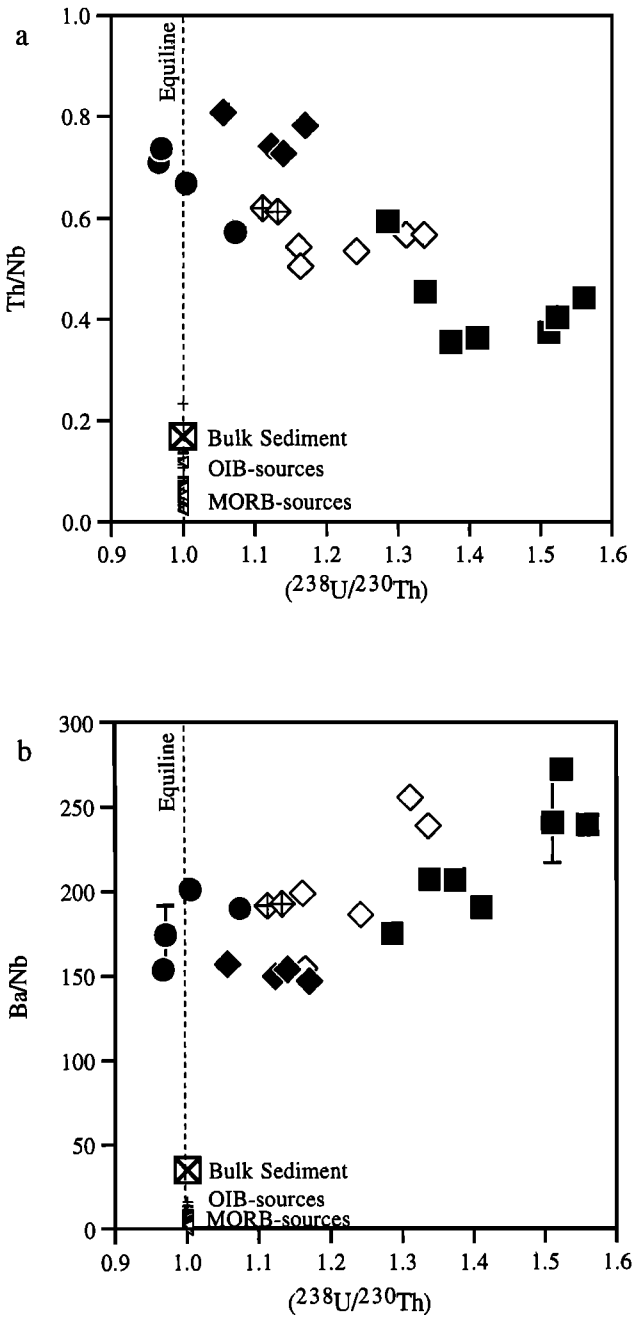

Figure 5. The ($^{238}U/^{230}Th$) versus (a) Th/Nb and (b) Ba/Nb for Mariana lavas of this study (symbols as Figure 2). MORB (left pointing open triangles) and Pacific OIB (crosses) sources are plotted, assuming incompatible element ratios are unfractionated during melting and that the sources are in secular equilibrium. The bulk Mariana sediment estimate from this study (crossed square) is also plotted assuming it is in equilibrium. High-precision Nb analyses on MORB are rare, especially in conjunction with other elemental data. Comprehensive elemental and isotopic data sets on the same OIB samples are also rather scant. For consistency, we use the same Pacific OIB and global MORB database throughout this paper (full references furnished on request). Error bars are plotted for two samples at either end of the compositional range of the Maraian lavas and are derived from the largest relative variation obtained from replicate analyses of several different samples. The errors thus to indicate maximum uncertainty, and in general, reproducibility is better than this. Reproducibility of ($^{238}U/^{230}Th$) is smaller than symbol size.

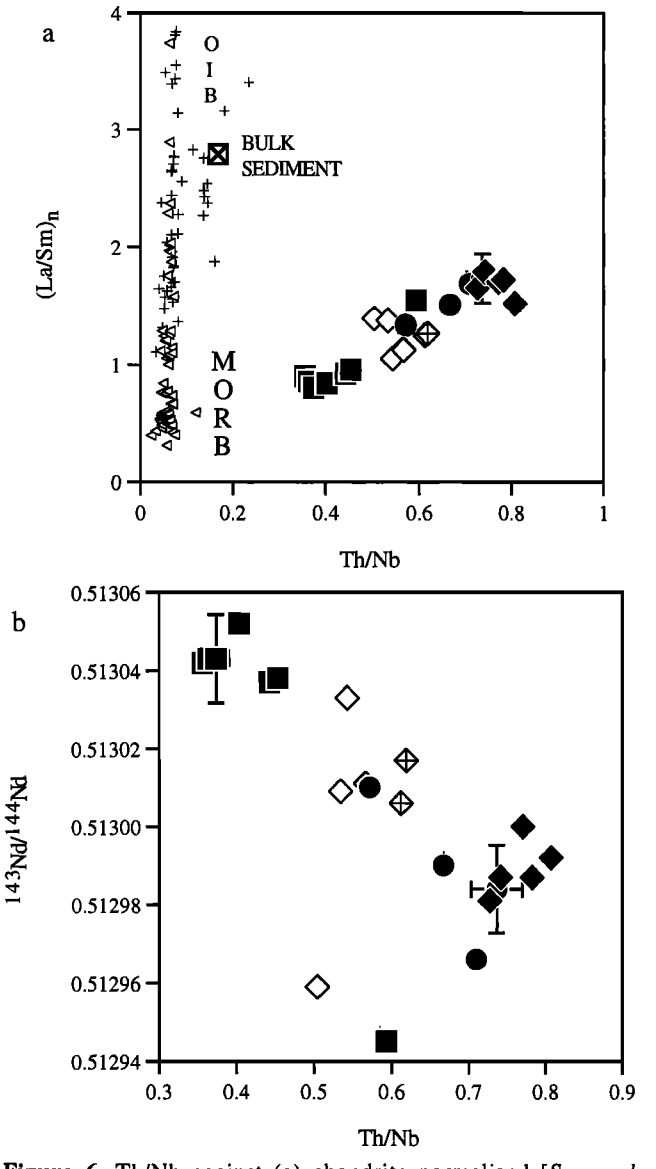

Figure 6. Th/Nb against (a) chondrite normalized [*Sun and McDonough*, 1989] La/Sm and (b) $^{143}Nd/^{144}Nd$ for the Mariana volcanics of this study (symbols as in Figure 2), together with MORBs (left pointing open triangles), Pacific OIBs (crosses), and Mariana bulk sediment (crossed square). No MORB or OIB data are shown in Figure 6b as this would compress the scale and mask the small, but significant variations within the Mariana lavas of this study. Error bars represent 2σ standard deviation of replicate analyses.

excesses, negative niobium anomalies and relative alkaline earth enrichments are all highly distinctive features of arc lavas [*Gill*, 1981; *Hawkesworth et al.*, 1991]. Both Ba/Nb and Th/Nb of all the lavas are significantly higher than any MORB or OIB (Figure 5). However, it is clear that elevated Ba/Nb and Th/Nb cannot be caused by the same process. Relative enrichment of Ba appears to be associated with production of large ^{238}U excesses (Figure 5b), while another mechanism is required to generate the lavas with the highest Th/Nb that have very little disequilibrium. It is instructive to see how the ratios plotted in Figure 5 correlate with other tracers. Since all three ratios are interrelated, we focus on Th/Nb which has the greatest relative variation. High Th/Nb ratios reflect the char-

acteristic negative niobium anomalies of arc lavas, independent of any alkali or alkaline earth enrichment, and so throughout the rest of the paper we use high Th/Nb and negative niobium anomalies synonymously.

Th/Nb shows a striking positive correlation with La/Sm (Figure 6a), such that Agrigan and Uracas lavas, with the largest niobium anomalies, also show the greatest light rare earth enrichments, in addition to highest absolute contents of many incompatible elements (Figures 2 and 3). Such enrichment is also reflected in small, but significant variations of $^{143}Nd/^{144}Nd$ (Figure 6b). Incompatible HSFE element ratios also correlate with Th/Nb (Figure 7), but even the most enriched Mariana lavas (i.e., highest Th/Nb) have Zr/Nb ratios as depleted as many MORB. This is in keeping with the very low Nb abundances of the Mariana lavas, which are as low as undifferentiated MORB (Figs. 2b and 2c). The variations in Ta/Nb are striking (Fig. 7b), as this ratio has been found to be constant and chondritic for a wide range of mantle derived materials [*Jochum et al.*, 1986, 1989].

An inverse variation of Ba/La with La/Sm is evident in the subaerial Mariana lavas (Figure 8a). Such a relationship has been previously reported for a number of other arcs [e.g., *Kay*, 1980; *Arculus and Powell*, 1986] and is also apparent in a sample set from a much longer segment of the Mariana arc [*Lin et al.*, 1989]. More generally, *Hawkesworth et al.* [1993a] observed that in a global compilation of mafic arc lavas, the most depleted lavas (least light rare earth enriched) exhibited the highest LILE/HFSE and LILE/REE ratios. Thus the processes that produce intra-arc variations within the Marianas may be common to many other arcs. The light rare earth depleted, low Th/Nb lavas of Guguan not only have the highest Ba/La and Ba/Nb but also other elevated LILE/REE and LILE/HSFE ratios, e.g., Figure 8b. Yet, despite having much larger ^{238}U excesses than the Agrigan lavas, the Guguan lavas have lower U/Nb (Figure 8c), although all Mariana lavas have significantly higher U/Nb than the near constant value of MORB and OIB [*Hofmann et al.*, 1986].

Radiogenic isotopic variations within the lavas of this study are minor compared to the range in incompatible trace element contents and ratios. The $^{87}Sr/^{86}Sr$ and $^{143}Nd/^{144}Nd$ ratios are slightly higher and lower, respectively, than MORB (Figure 9a). Unlike many of the incompatible element ratios discussed above, $^{87}Sr/^{86}Sr$ and $^{143}Nd/^{144}Nd$ compositions of the Mariana lavas overlap with OIB compositions, as emphasised by *Lin et al.* [1990]. Lead isotope ratios are fairly radiogenic and, as previously noted by *Woodhead and Fraser* [1985], form a slightly oblique trend away from Pacific MORB compositions toward the local sediment composition (Figures 9b and 9c).

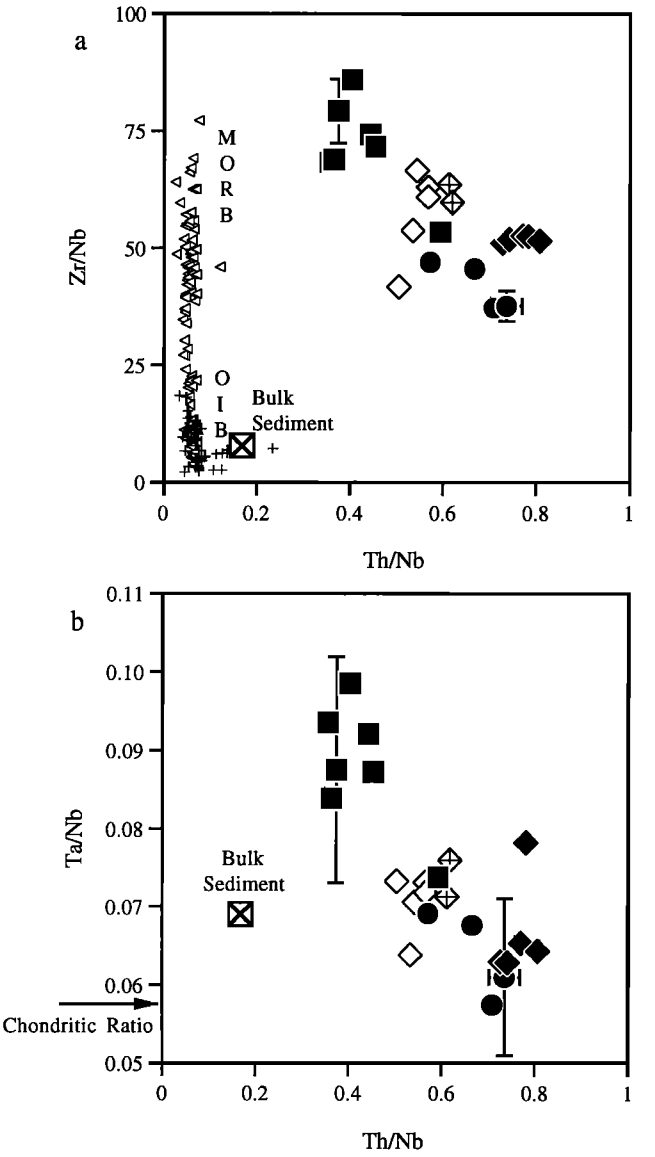

Figure 7. Th/Nb for the Mariana volcanics of this study (symbols as in Figure 2) plotted against (a) Zr/Nb and (b) Ta/Nb. Analyses of bulk Mariana sediment are shown, together with MORB and OIB compositions in Figure 7a, symbols as in Figure 6. MORB and OIB are not plotted in Figure 7b due to paucity of high precision data for Ta/Nb ratios. However, Ta/Nb ratios are generally assumed to be chondritic for all MORB and OIB samples, and therefore the chondritic Ta/Nb of *Sun and McDonough* [1989] is marked on the ordinate. Error bars, as described for Figure 5, indicate maximum uncertainty, and in general, reproducibility is better than this.

Discussion

Two Slab Components in Mariana Arc Magmas

Mafic arc lavas are thought to be produced by melting of the subarc mantle [e.g., *Ringwood*, 1974], yet, as is typical of most arc volcanics [*Gill*, 1981; *McCulloch and Gamble*, 1991; *Hawkesworth et al.*, 1993a] the Mariana lavas have many incompatible element ratios that are very different from any MORB or OIB (Figures 5-8). The covariations of some of these key element ratios provide insights into the processes responsible for creating these characteristic arc signatures. For example, as discussed above, whatever causes the large ^{238}U excesses cannot also create the most extreme Th/Nb (Figure 5a). Thus (at least) two independent processes must be at work in the Mariana subarc mantle. In the following section we discuss, in turn, what processes are likely to be responsible for producing the high ^{238}U excesses and Th/Nb, respectively.

Before discussing our new data, it is worth recapping previous models for the petrogenesis of Mariana lavas. Two main candidates have been invoked as the cause of light rare earth enrichment and lower $^{143}Nd/^{144}Nd$ of the more enriched lavas.

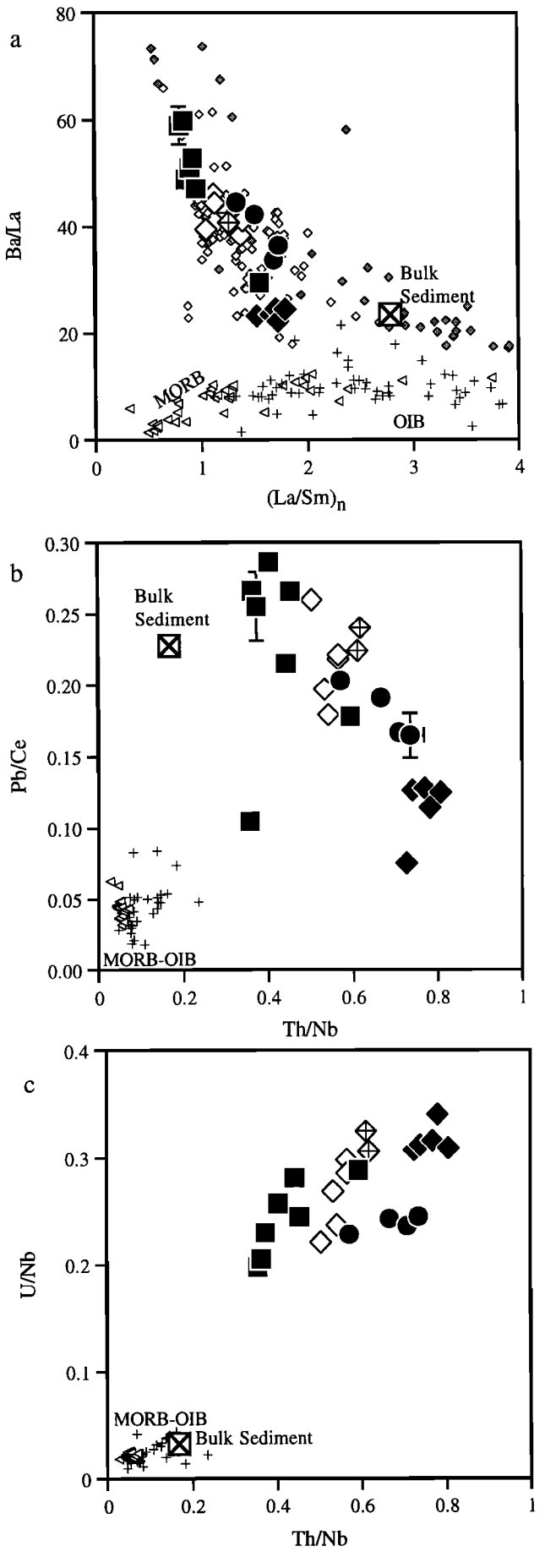

From this study it is apparent that this process must also produce high Th/Nb and other associated incompatible element ratios. Stern and coworkers [*Stern and Ito*, 1983; *Ito and Stern*, 1985/1986; *Stern et al.*, 1988; *Lin et al.*, 1990; *Lin*, 1992] have argued for a subarc mantle that is variably enriched with OIB-like material. *Lin et al.* [1990] further suggest that the range of Mariana lava compositions evident on a plot such as Ba/La versus La/Sm (Figure 8a) reflects mixing between a MORB-like mantle source that has been metasomatized by a high Ba/La slab-derived "fluid" component and OIB-type mantle with high La/Sm. In contrast, Woodhead and coworkers [*Woodhead and Fraser*, 1985; *Woodhead et al.*, 1987; *Woodhead*, 1989] implicate the role of sediment in the Mariana source and argue that prior to sediment addition the subarc mantle was MORB-like but further depleted by recent melt extraction [*Woodhead et al.*, 1993]. High LILE/LREE ratios in the lavas are argued to partly result from fractionation of the sedimentary material during its transport from the slab to the subarc mantle source [*Woodhead*, 1989].

Aqueous Fluid Addition

Mariana lavas with the largest ^{238}U excesses also have the highest Ba/Nb (Figure 5b) and Ba/La. The latter are indices that have been widely used as indicators of an aqueous fluid contribution from the slab [e.g., *Gill*, 1981; *Pearce*, 1982; *Lin et al.*, 1990; *McCulloch and Gamble*, 1991; *Hawkesworth et al.*, 1993a]. Serpentine dehydration experiments [*Tatsumi et al.*, 1986] and a number of recent high-pressure and temperature aqueous fluid-mineral partitioning experiments [*Brenan et al.*, 1995a; *Brenan et al.*, 1995b; *Keppler*, 1996] indeed suggest that fluids derived from slab dehydration should have high LILE/HSFE and LILE/LREE. Under normal mantle redox conditions [e.g., *Ballhaus et al.*, 1990; *Wood et al.*, 1990], Th and U are both tetra-valent, have similar geochemical behavior and are difficult to fractionate [*LaTourette and Burnett*, 1992; *Beattie*, 1993; *Lundstrom et al.*, 1994]. However, in more oxidizing conditions, such as suggested for subduction zones [*Ballhaus et al.*, 1990; *Wood et al.*, 1990], U can become hexa-valent and so may preferentially partition into aqueous fluids relative to Th [*Brenan et al.*, 1995a]. Hence addition of an oxidising aqueous fluid from the subducted slab can readily explain both ^{238}U excesses and high Ba/Nb in the Mariana mantle wedge and, consequently, in the magmas derived from it.

Figure 8. (opposite) (a) Chondrite normalized La/Sm [*Sun and McDonough*, 1989] versus Ba/La, (b) Th/Nb versus Pb/Ce and (c) Th/Nb versus U/Nb for the Marianas lavas of this study together with MORB, OIB, and bulk Mariana sediment compositions (symbols as in Figures 2 and 6). For the elements plotted in Figure 8a there are data available from others studies of the Mariana arc to show in comparison. Additional data from the Central Island province [*Dixon and Batiza*, 1979; *Meijer and Reagan*, 1981; *White and Patchett*, 1984; *Woodhead*, 1989] are plotted as small, open diamonds and data from other parts of the Mariana arc [*Lin et al.*, 1989], most notably the enriched lavas from the Northern Seamount province, are shown as small, shaded diamonds. Pb/Ce and U/Nb in Figures 8b and 8c, respectively, are inverse of the ratios found by *Hofmann et al.* [1986] to be near constant for all MORB and OIB samples. The Mariana lavas show striking deviations from these compositions.

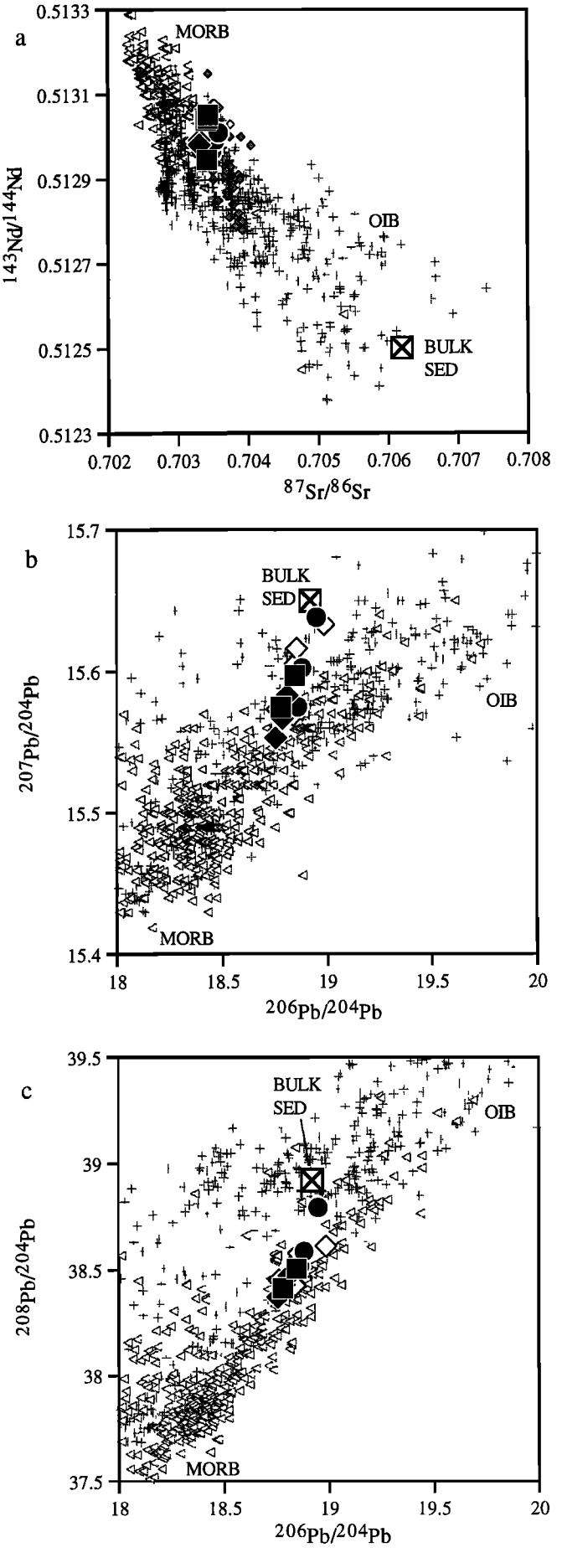

The importance of slab-derived "fluids" in accounting for large ^{238}U excesses and extreme LILE/HSFE enrichments in arcs comes from the observation that these signatures are most marked in the most depleted arc lavas. In mantle wedges that are strongly depleted in incompatible elements, the addition of a U (and LILE)-enriched aqueous fluid will have a significant leverage on the total U (and LILE) budget of the source and so produce large ^{238}U excesses (and high LILE/HSFE ratios). In contrast, the effect of a similar amount of fluid-derived U will be smaller in more enriched portions of the subarc mantle. Hence fluid mobile element concentrations are somewhat buffered by fluid addition, and this helps explain the smaller relative variations in Ba concentrations of the Mariana lavas compared to Th (Figure 2).

The production of large ^{238}U excesses in arc volcanics is not readily explained by processes other than addition of U-rich fluids. For example, very small degrees of melting would be required to significantly fractionate U-Th by mantle melting [e.g., *LaTourette and Burnett*, 1992; *Beattie*, 1993; *Lundstrom et al.*, 1994]. Not only are such small degrees of melting unlikely from major element constraints [*Plank and Langmuir*, 1988], but if ^{238}U excesses were produced by melting, the largest degrees of disequilibrium would be expected in the smallest degree melts with the highest incompatible element abundances and not the converse, as is the case for this study (see also *McDermott and Hawkesworth* [1991] and *Condomines and Sigmarsson* [1993]). The role of more complex melting processes has been invoked to explain ^{230}Th-excesses at large degrees of melting beneath mid-ocean ridges [e.g., *McKenzie*, 1985], but even if applicable to arcs, such models should produce vertical arrays on the equiline diagram rather than the near horizontal trend seen in Figure 4a.

Thus, beneath the Marianas, it seems most reasonable to explain the range of ^{238}U-^{230}Th disequilibrium as being due to the addition of a U-enriched aqueous fluid to a variably enriched (or depleted) mantle wedge. The amount of fluid added cannot vary randomly along arc or otherwise the inverse correlation with fluid-immobile indices (such as Th/Nb, Figure 5a) would be destroyed. The array of Mariana lava data is consistent with a be roughly constant fluid flux along the length arc. As noted earlier, the inverse variation of both ^{238}U excesses and LILE/HSFE ratios with indices of enrichment in the Marianas mimics what is observed in arc lavas globally. Likewise, many other studies have attributed the high ^{238}U ex-

Figure 9. (opposite) (a) $^{87}Sr/^{86}Sr$ versus $^{143}Nd/^{144}Nd$, (b) $^{206}Pb/^{204}Pb$ versus $^{207}Pb/^{204}Pb$ and (c) $^{206}Pb/^{204}Pb$ versus $^{208}Pb/^{204}Pb$ for the Mariana volcanics of this study together with MORB, OIB and bulk Mariana sediment compositions (symbols as in Figures 2 and 6). Also shown in Figure 9a are additional data from the Central Island province [*Dixon and Stern*, 1983; *White and Patchett*, 1984; *Woodhead*, 1989], small, open diamonds and other parts of the Mariana arc [*Stern and Bibee*, 1984; *Lin et al.*, 1990], small, shaded diamonds, most notably the highly enriched lavas from the Northern Seamount province. The large number of MORB and OIB samples plotted reflect the greater number of radiogenic isotope measurements in the literature relative to complete incompatible element analyses. The fuller isotopic database is used to give an indication of the distribution of isotopic compositions, rather than show the more restricted MORB and OIB compilations of samples with trace element and isotopic analyses that are used in all other figures

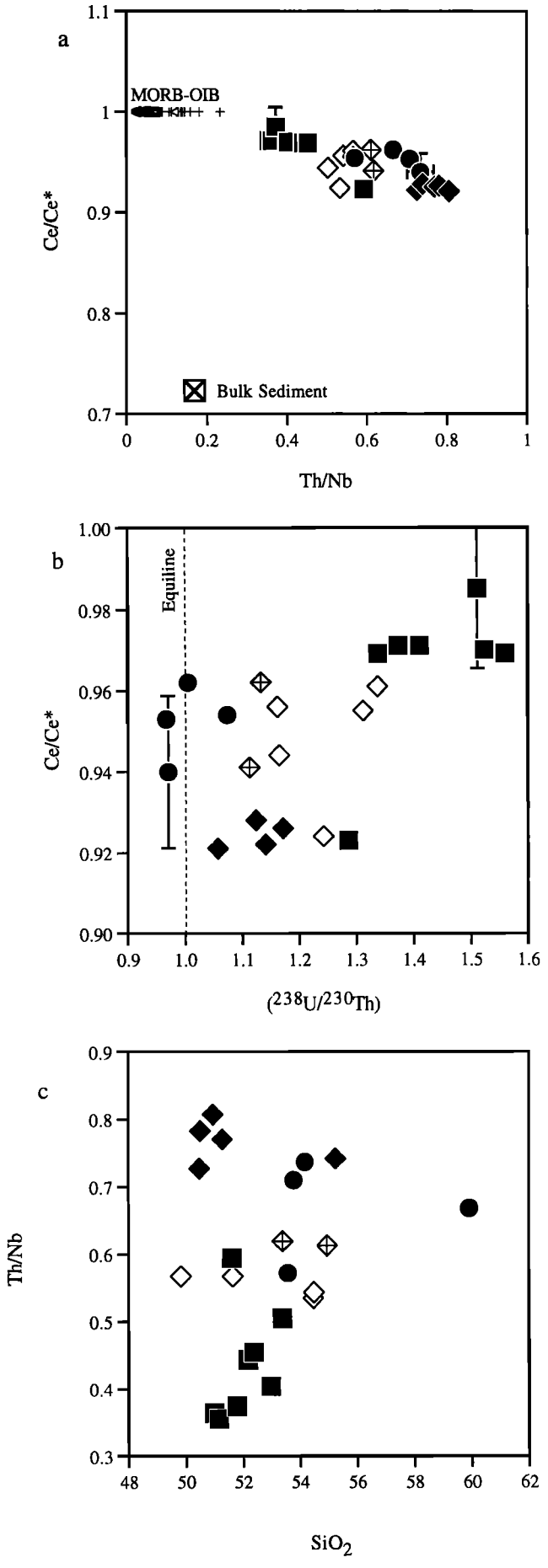

cesses and LILE/HSFE ratios of the depleted arc lavas to addition of a U and LILE rich slab fluid to their subarc mantle source [e.g., *Gill*, 1981; *Hawkesworth et al.*, 1993a, and references therein].

Enrichment of Fluid Immobile Elements

The enrichment process in the Mariana mantle wedge significantly increases Th/Nb as well as both Th and Nb concentrations (Figure 2b). Lavas with the highest Th/Nb also are the most light rare earth enriched and have lower $^{143}Nd/^{144}Nd$ (Figure 6). A further telling feature of the enrichment process is that lavas with highest Th/Nb also have the most marked negative cerium anomalies (i.e., $Ce/Ce^*<1$) (Figure 10a). *Woodhead* [1989] noted a comparable correlation of $^{143}Nd/^{144}Nd$ with Ce/Ce^* in his suite of subaerial Mariana lavas.

Ce/Ce^* is a ratio of the measured Ce concentration over the expected Ce concentration, calculated from interpolation of the chondrite-normalized abundances of its rare earth element neighbors, La and Pr. Under oxidizing conditions, a significant fraction of Ce is in the tetra-valent state and is fractionated from the other largely tri-valent rare earths. For example, seawater has a prominent negative cerium anomaly which is balanced by the positive cerium anomalies of some manganese nodules and Fe-Mn flocs [*Piper*, 1974; *Elderfield et al.*, 1981]. Slowly accumulating pelagic clays with abundant fish-debris apatite inherit seawater's negative anomaly [*Toyoda et al.*, 1990], and some Pacific pelagic clays are quite striking in their prominent negative cerium anomalies (Table 2) [*Hole et al.*, 1984; *Ben Othman et al.*, 1989; *Lin*, 1992].

We argue that the features observed in Figure 6, and more particularly in Figure 10a, strongly suggest that variable enrichment of the Mariana mantle wedge is achieved by variable addition of a subducted sedimentary component. The bulk sediment subducted beneath the Marianas has low $^{143}Nd/^{144}Nd$ (Figure 9a), is strongly light rare earth enriched (Figure 6a), and importantly has both a marked Ce anomaly and a small Nb anomaly (Figure 10a). Admittedly, bulk Mariana sediment does not have a sufficiently large Nb anomaly to be able to account for the composition of the Mariana lavas by bulk mixing with the subarc mantle (e.g., Figures 6 and 7). However, it is widely acknowledged that certain incompatible element ratios may be fractionated during transport of sedimentary material into the mantle wedge, and this is discussed in detail below.

Can the variable enrichment observed in the Mariana lavas be reasonably explained in ways other than the addition of a subducted sedimentary component? As mentioned earlier, Stern and coworkers [*Stern and Ito*, 1983; *Ito and Stern*, 1985/1986; *Stern et al.*, 1988; *Lin et al.*, 1990; *Lin*, 1992] have proposed that the Mariana lavas represent a dominantly two-component mixture between a low $^{143}Nd/^{144}Nd$ OIB-type

Figure 10. (opposite) (a) Th/Nb versus Ce/Ce^* (cerium anomaly is the deviation of Ce/Ce^* from unity; see text for further details), (b) $(^{238}U/^{230}Th)$ versus Ce/Ce^*, (c) SiO_2 (weight percent) versus Th/Nb for the lavas of this study (symbols as in Figure 2). Also shown in Figure 10a are MORB, OIB (assumed to have no Ce anomaly), and bulk Mariana sediment compositions (symbols as in Figure 6). Error bars, as described for Figure 5, indicate maximum uncertainty, and in general, reproducibility is better than this.

mantle and a high $^{143}Nd/^{144}Nd$ MORB-type mantle metasomatized by a slab-derived, LILE-rich fluid. Their model is unable to explain many of the observations of our data set, as the low $^{143}Nd/^{144}Nd$ component requires some incompatible element ratios (e.g., Th/Nb, Ce/Pb, Ce/Ce^*, U/Nb) that are quite unlike those of any OIB. If an OIB component is the chief incompatible element contributor to the enriched lavas, it must have been highly fractionated to suitably change these incompatible element ratios. This however begs the question, can we distinguish a fractionated sediment component from a fractionated OIB contribution to the subarc mantle?

Although we argue that some elemental fractionations are required for the subducted sediment to become a suitable enriched component, many of the key incompatible element features are already evident to some extent in the bulk sediment itself. Significantly, the bulk sediment has negative niobium (Figure 3) and cerium anomalies (Figure 10a) prior to subduction, not to mention low Ce/Pb and Nb/U (Figures 8b and 8c). As we detail later, it is difficult to generate an enriched end-member with suitably high Th/Nb, even starting with an existing negative niobium anomaly, as in the bulk sediment. To do this from an OIB source, which generally have positive niobium anomalies is even more problematic. Thus while subducted sediment requires fractionation of some element ratios to become a suitable end-member for Mariana lavas, greater fractionations of more ratios would be required starting from an initial OIB source.

Producing negative cerium anomalies from a putative OIB source is also difficult to explain. Although *White and Patchett* [1984] argued that negative Ce anomalies may result from contrasting partitioning of REE into an oxidising aqueous fluid from slab dehydration, data from this study argue against this as an effective mechanism. If such a process did operate, then large cerium anomalies would be associated with other signatures of the oxidised fluid, such as the large ^{238}U excesses and high Ba/La. However, the Guguan lavas with the greatest ^{238}U excesses and Ba/La in fact have the smallest cerium anomalies, i.e., Ce/Ce^* closest to unity (Figure 10b). This implies that the negative cerium anomalies are characteristic of the enriched component itself (like the subducted sediment) and not a product the process by which it was transferred.

While many of the Marianas lavas plot within the OIB lead isotope field, in detail only a small fraction of analyzed OIB have similar lead isotope ratios to the Mariana lavas (e.g., Figure 9b). Thus the model of Stern and coworkers requires a rather specific OIB source. However, bulk subducting sediment at the Mariana Trench plots at the end of lead isotope array of the Mariana lavas (Figure 9) and so can readily account for their lead isotopic compositions. *Woodhead* [1989] illustrated a strong coherence of the lead isotopic composition of arc lavas and the very different compositions of subducted sediment worldwide, and similar systematics have been observed on a local scale [*White and Dupré*, 1986; *McDermott et al.*, 1993; *Vroon et al.*, 1995]. Likewise, it is striking that cerium anomalies in arc lavas and subducted pelagic sediment are restricted in their global occurrence, but both are prominent in the western Pacific [*White and Patchett*, 1984; *Ben Othman et al.*, 1989; Plank and Langmuir, submitted manuscript, 1996]. If cerium anomalies were produced by a common arc fractionation process, it would be expected they would be a much more usual feature of arc lavas. While it is very difficult to unequivocally disprove the involvement of a fractionated, arbitrarily selected OIB composition in any specific arc locality, we feel that the association of key geochemical signatures in the Mariana lavas and the adjacent subducting sediments is more than mere coincidence.

If the mantle reaction models of Kelemen and coworkers [*Kelemen et al.*, 1990, 1993] were invoked to explain the range of Mariana lava compositions, variable amounts of reaction between percolating melt and the subarc mantle matrix would be required. These models predict decreasing Nb concentrations with increasing Nb anomaly, which is the opposite to what is observed in Figure 2b. Moreover, larger amounts of melt percolation through a depleted upper mantle would also be expected to produce the highest $^{143}Nd/^{144}Nd$ in the lavas with the highest Th/Nb. This is again the opposite to what is observed in the Mariana lavas (Figure 6b).

Crustal contamination may create enrichment in erupted arc lavas that is unrelated to the mantle source [e.g., *Davidson*, 1987; *Hildreth and Moorbath*, 1988]. It is stressed that the opportunity for crustal contamination at the Marianas is small compared to other arcs, as largely mafic lavas are erupted through oceanic crust. Nevertheless, crustal interaction of some sort may still occur. However, if contamination were the dominant cause for enrichment in the Mariana lavas, it might be expected that this enrichment would correlate with an index of magmatic differentiation. As is clear from Figure 10c, this is not the case in the Marianas. The full range of incompatible trace element ratios for the subaerial lavas are apparent within the least evolved samples. For individual islands (e.g., Agrigan), a large range of SiO_2 is apparent with minor or no variation in incompatible element ratios (Figure 10c).

Hence we argue that the variable enrichment observed in the Mariana arc is most plausibly explained by variable enrichment of the subarc with a subducted sedimentary component. The striking negative correlations of ^{238}U excesses with Th/Nb (and Ba/La with La/Sm), result from the independent addition of a slab derived aqueous fluid to this variably enriched subarc mantle. Such a model is thus similar to previous three component models [*Kay*, 1980; *Ellam and Hawkesworth*, 1988; *McDermott et al.*, 1993; *Plank*, 1993; *Miller et al.*, 1994; *Turner et al.*, 1996]. In the following sections we investigate these processes in more detail, but first, we examine the nature of the subarc mantle prior to modification by subduction-related components.

Composition of the Unmodified Subarc Mantle

Although it is argued that the Mariana lavas represent melts of a mixture of mantle, sediment contribution, and aqueous fluid, the problem can be reduced to a simpler two-component mixing problem by only considering elements that are not carried in the aqueous fluid. In plots of fluid immobile incompatible elements, the Mariana volcanics display arrays (e.g., Figures 6 and 7) that we infer to reflect variable mixing of a sediment component with a depleted mantle wedge. We argue that the lavas with lowest Th/Nb (which also correlate with the other indices of enrichment) are derived from sources with the least sediment addition, and so most closely resemble unmodified subarc mantle. However, it is clear that the most depleted Mariana lavas still have Th/Nb ratios significantly higher than any MORB or OIB composition (Figure 6a), and so we suggest that even the depleted sources have experienced sufficient input of high Th/Nb sedimentary material to perturb their composition.

Previously authors have used HSFE to examine the composition of unmodified subarc mantle [*McCulloch and Gamble*, 1991; *Woodhead et al.*, 1993]. This approach has the advantage that subducted sediment is generally less enriched in HSFE than Th or LREE (i.e., has a negative Nb anomaly), and so HSFE ratios of the subarc mantle will be relatively less affected by the process of sediment addition than ratios involving Th and LREE. As noted earlier, lavas derived from sources with the least sediment addition (i.e., lowest Th/Nb) have more depleted Zr/Nb than any published MORB, and they also have nonchondritic Ta/Nb (Figure 7b). Our results thus amplify the work of *Woodhead et al.* [1993], who used less highly incompatible, fractionation-corrected HSFE element ratios in arc lavas to infer a highly depleted unmodified mantle beneath many subduction zones. Highly depleted mantle xenoliths have also been reported in some arc lavas [*Maury et al.*, 1992].

The non-chondritic Ta/Nb ratios place useful constraints on the nature of the depletion process [*Plank et al.*, 1994; *Plank and White*, 1995; *Stolz et al.*, 1996]. Although Ta is more compatible than Nb in "normal" mantle assemblages [*Green et al.*, 1989; *Forsythe et al.*, 1994], both elements are highly incompatible and so very difficult to fractionate by most magmatic processes. However, even highly incompatible elements can be fractionated in mantle residues that have experienced fractional melt extraction. Studies of abyssal peridotites [*Johnson et al.*, 1990], as well as basalts [*Langmuir et al.*, 1992], have argued that melt production beneath ridges is a near fractional process. Thus the HSFE ratios of the Mariana lavas implicate the presence of a subarc mantle that was previously depleted by a fractional melting event, as occurs beneath mid-ocean ridges. Such melt depletion of the mantle wedge seems likely to occur during backarc spreading [*McCulloch and Gamble*, 1991; *Woodhead et al.*, 1993].

The evidence for backarc depletion of the unmodified Mariana mantle source provides further arguments against the likelihood of OIB material significantly participating in Mariana arc magmatism. Any fertile, OIB-like blebs are likely to be melted out during backarc spreading, prior to mantle entrainment into the subarc region. It might also be expected that such enriched components would thus be more clearly evident in the backarc crust than in the arc lavas, whereas the reverse is true [*Volpe et al.*, 1987; *Stolper and Newman*, 1994]. Conversely, prior melt depletion of the subarc mantle makes it highly susceptible to additions of incompatible element rich sediment from the subducted plate.

Process of Sediment Addition to Subarc Mantle

In attempting to constrain the composition of the added sedimentary component, we adopt a similar approach as in the last section but focus on the enriched rather than depleted end-member of the Mariana sample arrays. Thus we again only examine elements that are thought to be largely fluid immobile. Two-component mixing arrays should be linear in the plots of Th/Nb versus La/Nb and $^{143}Nd/^{144}Nd$ versus La/Nd (Figures 11a and 11b), and since no straight line emanating from the bulk sediment toward any unmodified mantle composition can adequately reproduce the trend in the Mariana volcanics, we reaffirm the earlier observation that bulk sediment cannot be the enriched end-member.

It is initially necessary to assess the reliability of our bulk sediment estimate. Hole 801, out-board of the Marianas, is well studied petrologically and chemically [*Lancelot et al.*, 1990]. *Plank and Ludden* [1992] have shown that due to the coherency between sediment geochemistry and lithology, reliable bulk estimates can be made from a few representative samples of such a well characterised section. It is perhaps more likely that errors in the composition of sedimentary input could lie in variations in thickness of the main sedimentary units. Seismic imaging suggests no major discontinuities in the sediment structure off the Mariana trench [*Shipley et al.*, 1983; *Abrams et al.*, 1992], but there are some variations in the thicknesses of volcaniclastic units [*Lancelot et al.*, 1990]. Selective removal of the upper sedimentary units beneath the forearc could also change the effective mean sedimentary composition that is subducted to depth.

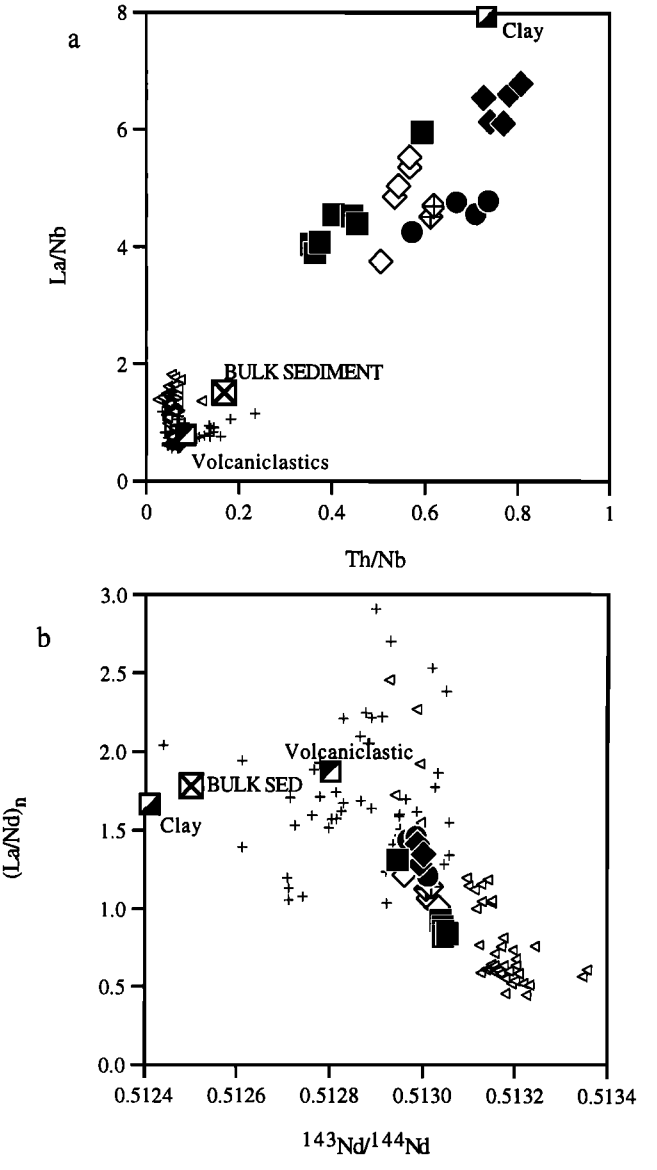

Figure 11. (a) Th/Nb versus La/Nb, (b) $^{143}Nd/^{144}Nd$ versus La/Nd (normalized to chondritic abundances of *Sun and McDonough* [1989]) for the Mariana volcanics (symbols as Figure 2), MORB, OIB (symbols as in Figure 6), and the principal components of the subducted Mariana sediment assemblage (bulk sediment, open crossed square; upper pelagic clay layer, half solid square; Cretaceous volcaniclastics, half solid square).

Such worries, however, can be readily addressed by investigating how the bulk sediment composition changes with varying the proportions of sedimentary units. This is a fairly straightforward exercise because, aside from the upper pelagic clay, the only major repository for the elements considered in this study is the volcaniclastic unit. The other main lithologic units, chert and radiolarite, are somewhat similar in composition to the pelagic clay, but severely diluted by biogenic silica (Table 2). Thus, for most incompatible elements, variations in the bulk composition can be modelled grossly as a two component mix. As can be seen in Figures 11a and 11b, simply altering the proportions of the two principal sedimentary components does not result in a suitable bulk sediment end-member for the Mariana array. For example, a sediment component consisting only of the upper clay layer would almost be a suitable enriched end-member to mix with a MORB source to account for the array of lavas in Figure 11a. However, when considering other elements, pure clay can be seen to be an unsuitable mixing end-member (Figure 11b). Thus simply varying the proportions of the sedimentary units in the subducted component cannot alone produce an appropriate enriched end-member, although this may explain second-order geochemical variations, as discussed later.

In order to be able to reproduce the Mariana lava array by mixing of subducted sedimentary material with depleted MORB, the added sedimentary component is required to have higher La/Nd and very significantly greater Th/Nb and La/Nd than the bulk sediment composition (Figures 11a and 11b). Elemental fractionations associated with transport of sedimentary components from slab to the mantle wedge is an appealing mechanism to explain these observations. A liquid phase, whether a melt or aqueous fluid produced by sediment dehydration, is also perhaps the most plausible way to transfer efficiently sedimentary mass into the mantle wedge.

The trace element composition of a liquid phase will be controlled not only by the bulk sediment composition but also the nature of the liquid phase (aqueous fluid or melt) and the residual phase mineralogy of the subducted sedimentary assemblage. Thus models of the sediment transport process tend to be highly under-constrained. However, it is possible to glean some first order insights, that can help resolve whether or not a sediment derived melt or "fluid" is the agent of transport. The high-pressure mineralogy of pelagic sediment is likely to contain some of the following major mineral phases: mica, amphibole, coesite, kyanite, orthoclase, clinopyroxene and garnet [*Johnson and Plank*, 1993; *Nichols et al.*, 1994; *Irifune et al.*, 1994]. A melt or aqueous fluid in equilibrium with such an assemblage may quite plausibly have higher La/Nd than the bulk sediment [*Green*, 1994], as required by Figure 11b, but given available partition coefficients [e.g., *Green*, 1994; *Hauri et al.*, 1994; *Brenan et al.*, 1995a] the requisite, large Th/Nb and La/Nb fractionations are not anticipated, not even in the halogen rich fluid of *Keppler* [1996].

Trying to reproduce the extreme niobium anomaly required in the enriched end-member actually provides some independent constraints on the subarc processes. Since none of the major mineral phases mentioned above can readily achieve large Th-Nb fractionations, it is necessary to call upon the accessory mineral rutile, which has very high HSFE partition coefficients for both melts [*McCallum and Charette*, 1978; *Green and Pearson*, 1987; *Jenner et al.*, 1993] and aqueous fluids [*Brenan et al.*, 1994]. Experiments show that while mafic melts have a high rutile solubility, siliceous melts much more readily saturate in rutile [*Ryerson and Watson*, 1987]. Indeed, *Nichols et al.* [1994] report rare grains of rutile as a quench phase of their pelagic sediment melt.

Nevertheless, residual rutile alone is not sufficient to explain the required fivefold increase of Th/Nb and La/Nb in the sediment component relative to bulk sediment (Figure 11a). To achieve such fractionations, not only does Nb need to be significantly retained in the sediment residue, but La and Th must also be efficiently transported in the sediment fluid or melt. A simple, end-member mass balance calculation exemplifies the point. We allow all sedimentary titanium (Table 2) to form rutile and use the highest experimentally derived $D_{Nb}^{rutile/liquid}$ [*Jenner et al.*, 1993]. Choosing a likely minimum fraction of sedimentary derived liquid is problematic. However, at less than some 5% melt/fluid fraction, significant amounts of hydrous phases are might be present in the residue. This would result in high alkali and alkali earth distribution coefficients such that the liquid phase would have a problem imparting sufficiently high Ba/Nb to the enriched sources. In this best case scenario, the bulk distribution coefficients for Th and La between sediment residue and liquid still need to be less than 0.1.

Clinopyroxene and amphibole should have the largest partition coefficients for La and Th in the residual sediment assemblage (the additional presence of accessory phases such as apatite or monazite would make it yet more difficult to produce large increases of La/Nb and Th/Nb) and so should control their bulk distribution coefficients [*Green*, 1994]. Reassessment of old data and recent determinations of high-pressure and temperature LREE partitioning between clinopyroxene and aqueous fluid suggest that $D_{La}^{cpx/aqueous\ fluid}$ is not significantly less than 1 [*Brenan et al.*, 1995b; *Keppler*, 1996]. La should be at least as compatible in amphibole as in clinopyroxene [*Green*, 1994], and so it is difficult for a sediment-derived aqueous fluid to sufficiently fractionate La/Nb ratios relative to the bulk-sediment. Melts, however, partition most cations more strongly than aqueous fluids [*Brenan et al.*, 1995a] and, in fact, $D(LREE^{cpx/melt}) << D(LREE^{cpx/aqueous\text{-}fluid})$ [*Brenan et al.*, 1995b]. Thus the efficient transfer of the REE and Th to the mantle wedge appears to implicate a silicate melt as the agent of transport of sedimentary material. Admittedly there is some disagreement in the studies trying to constrain fluid-mineral partition coefficients inferred from different studies [c.f., *Keppler*, 1996; *Ayers and Eggler*, 1995], and so it may be necessary to reassess the need for a sediment melt once the results of studies converge. However, given the present experimental data, the compositional considerations of this study seem to require a melt in equilibrium with rutile, rather than an aqueous fluid as the transport agent for sedimentary material.

Variability in the Subducted Component

From the criteria so far discussed, the lavas of Agrigan and Uracas are both derived from a source that contains a relatively large amount of sediment (high Th/Nb and La/Sm, low $^{143}Nd/^{144}Nd$). However, compared to Uracas, the Agrigan lavas have notably less radiogenic Sr and Pb isotope ratios (Figure 9 and Table 1) and lower Pb/Ce (Figure 8b). Indeed, the Sr and Pb isotope ratios and Pb/Ce for the Agrigan lavas are some of the lowest of the whole Central Island province, which is not in keeping with a large contribution of high $^{87}Sr/^{86}Sr$, $^{206}Pb/^{204}Pb$ and Pb/Ce sediment to their source.

While the pelagic sediment thicknesses in the western Pacific are rather uniform [*Abrams et al.*, 1992], significant variability must be caused by the presence of the Magellan seamounts which are presently being subducted beneath the Marianas (Figure 1). The chemical impact of a subducted seamount and its volcanic apron can be expected to be very significant, being several kilometres thick as opposed to the five hundred meters of the pelagic sediment pile. The Magellan seamounts have variable radiogenic isotopic signatures, but many show Pb and Sr isotopic ratios [*Staudigel et al.*, 1991] suitably less radiogenic than the pelagic sediments. The Magellan volcaniclastics (like all OIB) also have much lower Pb/Ce than the bulk sediment (see Table 2), and so a greater seamount-volcaniclastic contribution in the bulk-subducted sediment could also account for the higher Ce/Pb of the Agrigan lavas relative to Uracas.

Composition and Relative Magnitude of the Aqueous-Fluid Flux

The array of Mariana lavas in Figures 6 and 7 can be reasonably inferred to lie on a mixing array between mantle and the sediment melt component, although in some of the diagrams, the array diverges into a fan due to small differences in composition of the sediment component (e.g., Figures 10a and 11a). Such simple systematics are only preserved for the fluid-immobile elements. As discussed earlier, for a near constant aqueous-fluid flux, sources with least sediment addition are most affected by aqueous-fluid addition, such that the sediment-poor end of Mariana array rotates away from a depleted-mantle composition to one with elevated LILE/HSFE or LILE/REE ratios. Hence, diagrams such as Figure 8 provide a qualitative way of assessing the relative importance of aqueous fluid compared to sediment component in budgets of different elements in the subarc mantle.

For example, enrichment of uranium relative to niobium, compared to near constant MORB-OIB values of 0.02 [*Hofmann et al.*, 1986], is rather more marked in lavas derived from sediment-rich sources of Agrigan than in the relatively aqueous-fluid-rich Guguan lavas, that show such spectacular ^{238}U excesses (Figure 8c). Thus, even though significant U enrichment is caused by addition of the aqueous fluid phase, it appears that sediment additions are more important in the total uranium budget of the subarc mantle. In contrast, enrichments of Ba and Pb (relative to Nb and La, for example) are most marked in the sediment-poor Guguan lavas (Figures 8a and 8b), indicating a major role of the aqueous-fluid phase in transporting these elements.

Isotopic evidence helps to further characterise the aqueous fluid. Since the Pb budget of the Guguan lavas is dominated by the aqueous fluid addition (Figure 8b), we can use the Pb isotope ratios of the Guguan lavas to infer the composition of the aqueous fluid phase. Similar arguments can be made for Sr isotope ratios. The $^{206}Pb/^{204}Pb$ ratio of the aqueous fluid is thus inferred to be ~18.8, while the $^{87}Sr/^{86}Sr$ ratio is around 0.7035. These ratios are maxima due to the additional small contribution of more radiogenic sedimentary material to the Guguan source. Although these isotopic ratios are a little high and low, respectively, for best estimates of altered MORB [*Meijer*, 1976; *Staudigel et al.*, 1995], they are not unreasonable and certainly do not bear any resemblance to a sedimentary signature. Thus, as with previous authors [e.g., *Miller et al.*, 1994], we infer that the aqueous fluid is most plausibly derived from dehydration of the altered oceanic crust.

Timing of Processes in the Subduction Zone

The ^{238}U-^{230}Th disequilibrium provides information on the timing of U-Th fractionation. We argue above that the addition of a slab-derived fluid to the mantle wedge is responsible for creating the ^{238}U excesses in the Mariana lava sources. That this excess is preserved in the erupted lavas reflects the short time between fluid addition and magma eruption. In fact, the extremely coherent, subhorizontal array of the Mariana lavas on the equiline (Figure 4a) places rather tight constraints on this timing. However, in order to quantify these constraints it is necessary to examine different possible interpretations of the Mariana array.

Addition of U to an old source (i.e., >350 ka and therefore in secular equilibrium) produces horizontal displacement on the equiline diagram, and subsequent ingrowth of ^{230}Th returns the sample to secular equilibrium (i.e., the equiline) along a vertical vector. This is illustrated for a single source composition in Figure 12a. In the case of the Marianas, as we have already discussed at length, there are a range of variably enriched sources. Addition of a constant flux of U from the aqueous fluid phase to sources that are variably enriched in U by prior sedimentary addition results in a horizontal array of fluid-enriched sources and their melts (Figure 12b). Any aging of the sources after aqueous fluid addition results in rotation of this zero-age isochron (Figure 12b). Thus in this model the slope of the array of lavas then simply reflects the time between fluid addition to the sources and eruption of the melts.

The model above implicitly assumes that the variably sediment enriched sources have identical ($^{238}U/^{232}Th$) ratios. Although this is not implausible (see below), it is also quite possible that there is coherent variation of U/Th with absolute U content in the variably sediment enriched sources. The scenario sketched in Figure 12c can hence be envisaged, in which more depleted sources might be expected to have lower Th/U, or higher ($^{238}U/^{232}Th$). As before, a uniform flux of U-rich aqueous fluid will induce greater disequilibrium in the more depleted sources, but in this case, the zero-age isochron has a finite slope (Figure 12c). It is also possible that the U-rich aqueous fluid also carries some Th. Although it has been argued that the Th budget is dominated by the sedimentary addition, the fluid phase may nevertheless carry enough Th so that mixing with an aqueous fluid may be along an oblique, not a horizontal, vector (Figure 12d). The exact slope of the array will depend on both Th content and ($^{230}Th/^{232}Th$) of the fluid.

However, regardless of the details of the chosen model, the very small spread in ($^{230}Th/^{232}Th$) of the Mariana lavas (excluding the Alamagan lavas) is remarkable. If the whole range in ($^{230}Th/^{232}Th$) is due to time elapsed since fluid addition (such as in Figure 12b), the inferred 30 kyr is still a small time window for melting, melt migration and any shallow level differentiation prior to eruption. For example, taking the 120 km depth to the Benioff zone [*Issacks and Barazangi*, 1977] as the distance for magma migration, and assuming all the other processes take negligible time, then melt velocities of some 4 m/yr are required. If any of the spread in ($^{230}Th/^{232}Th$) is attributed to other effects (Figures 12c and 12d), then the time allowed for melt migration is consequently even smaller. Thus independent of model variants, the time between aqueous-fluid addition and eruption is less than 30 kyr for all lavas (apart from at Alamagan).

Not only are ($^{230}Th/^{232}Th$) ratios of the Mariana lavas rather constant, but they are also fairly high, which translates into low Th/U ratios (see Figure 4) of the Mariana sources

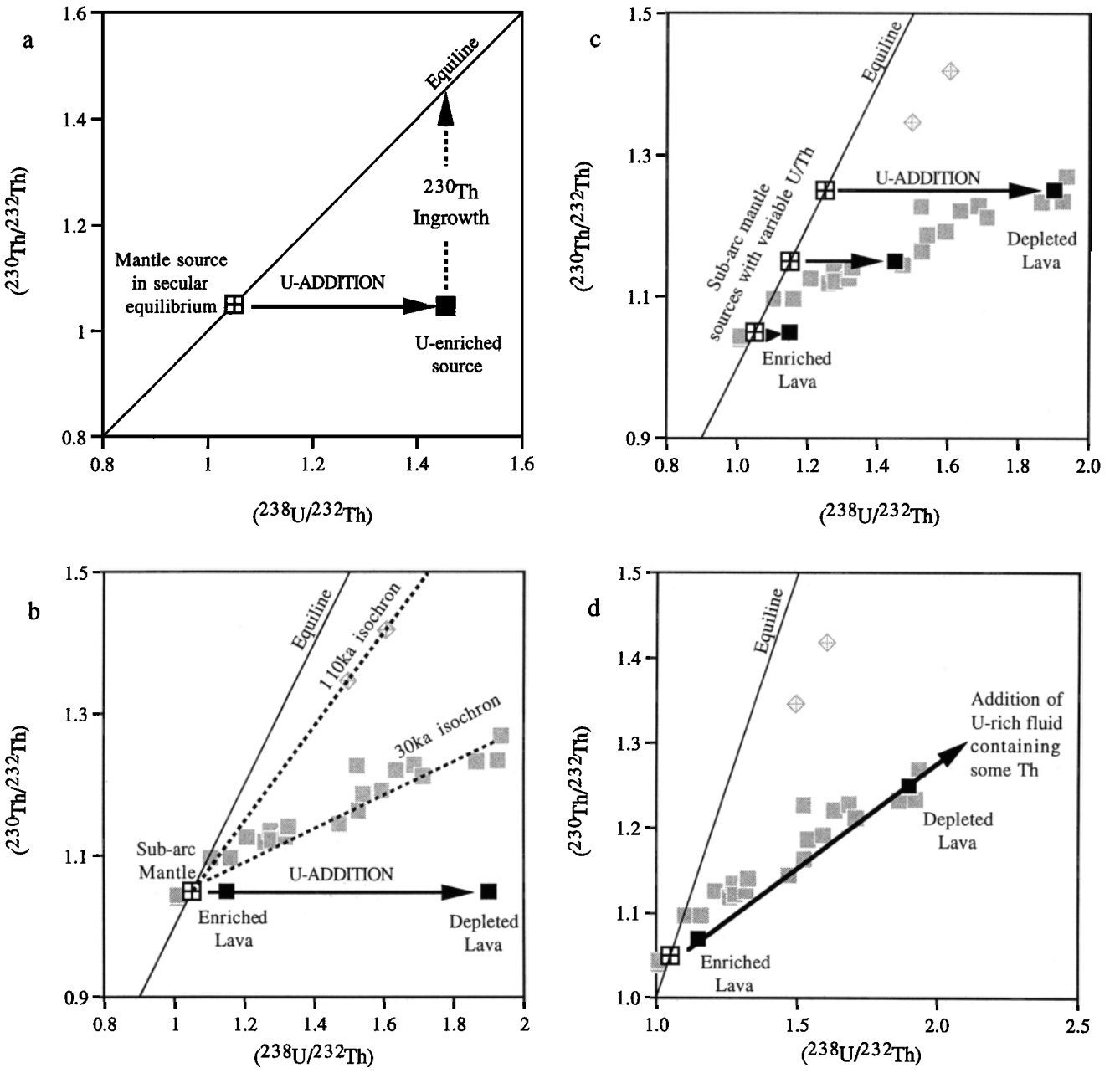

Figure 12. Equiline diagrams to illustrate the various possible effects of aqueous fluid U addition to a subarc mantle sources. (a) The basic systematics of an equiline diagram. Addition of U to a source initially in equilibrium moves it along a horizontal vector into disequilibrium (^{238}U excess), and then, with time, ingrowth of ^{230}Th returns the source to equilibrium, at higher ($^{238}U/^{232}Th$), along a vertical vector. (b) Variably enriched subarc mantle sources are assumed to be in equilibrium and have a range of absolute U contents but the same ($^{238}U/^{232}Th$). Thus initially the different sources plot on the same spot on the equiline diagram (open square with cross). However, addition of an equal amount of U-rich aqueous fluid has a greater effect on the U poor source, and this is illustrated with an enriched and depleted source after aqueous fluid addition (solid squares). The equiline plot is an isochron plot, and so these two points define a zero-age isochron. The Mariana lavas are shown as filled grey squares, and the bulk of the analyses can be interpreted as a ~30 ka isochron, while the two lavas from Alamagan appear to define a ~110 ka isochron with the same initial ($^{230}Th/^{232}Th$). (c) The effect of U addition to variably enriched subarc mantle sources in which ($^{238}U/^{232}Th$) varies inversely with the absolute U contents. Again the effect of a flux of U is greatest on the most depleted source, which in this case also has the highest ($^{238}U/^{232}Th$). Hence the zero-age array of aqueous fluid enriched sources (and their melts) is oblique and can mimic the array of the Mariana lavas without additional aging. (d) A variant of Figure 12b is illustrated where the added aqueous fluid is not only U-rich but also carries some Th. The slope of the resulting array after aqueous fluid addition will depend on ($^{230}Th/^{232}Th$) and ($^{238}U/^{232}Th$) of the fluid. As with the scenario shown in Figure 12c, this could feasibly mimic the compositions of Mariana lavas without additional aging after fluid addition.

prior to fluid addition. This is somewhat surprising, as the bulk-subducted Mariana sediment has high Th/U, and since it is presumably in secular equilibrium, low ($^{230}Th/^{232}Th$). Addition of such sediment to the highly depleted subarc mantle would impart low ($^{230}Th/^{232}Th$) to the arc lava sources. This is readily seen in curve A of Figure 13a, which plots some ($^{230}Th/^{232}Th$) and $^{143}Nd/^{144}Nd$ mixing calculations for sediment and a depleted mantle source. Since the sediment has high Th/Nd and the melt depleted mantle very low Th/Nd, the mixing trajectories are strongly hyperbolic. The amount of sediment addition required to affect even a small change in $^{143}Nd/^{144}Nd$ results in setting the ($^{230}Th/^{232}Th$) of the arc lava source to essentially that of the sediment (Figure 13a).

Thus the sedimentary component must have a ($^{230}Th/^{232}Th$) at least as high as the lowest value in the Mariana lava suite. This pins the mixing curve to go through the lower-most point of the $^{143}Nd/^{144}Nd$ array (curve B, Figure 13a). The rest of the variation in ($^{230}Th/^{232}Th$) can be attributed to ^{230}Th in-

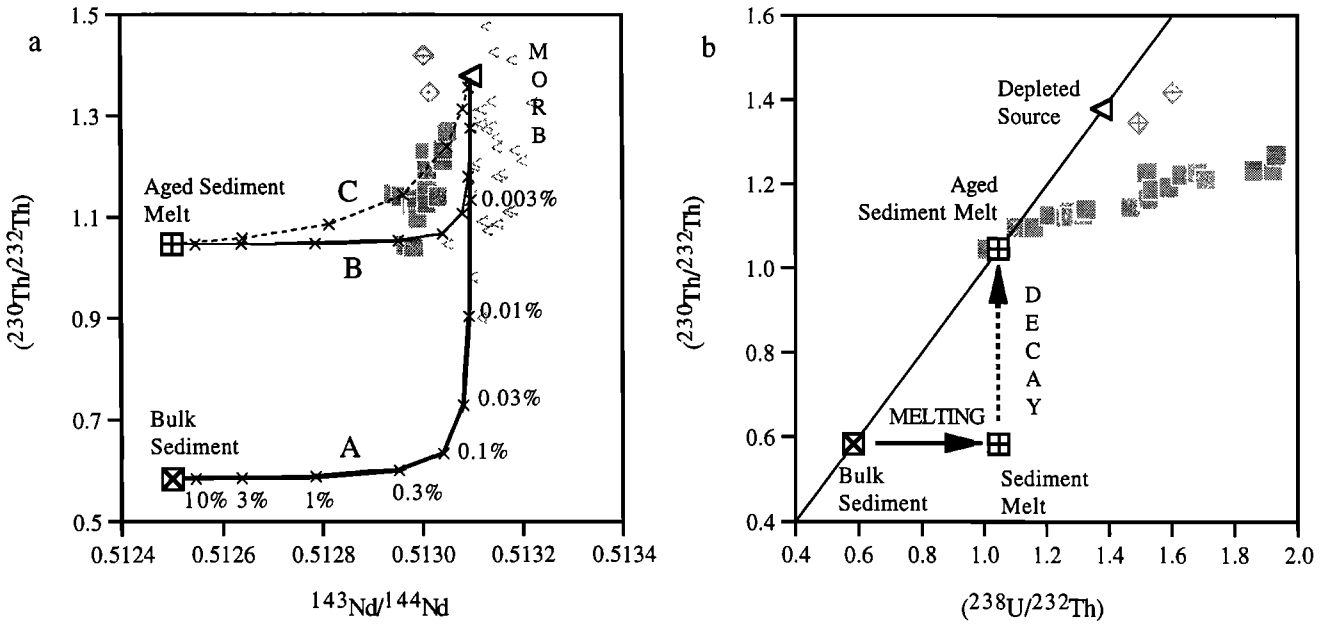

Figure 13. (a) $^{143}Nd/^{144}Nd$ versus ($^{230}Th/^{232}Th$) showing the Mariana lavas of this study (grey filled squares, except Alamagan samples which are shown as crossed diamonds), bulk Mariana sediment (diagonally crossed square), proposed composition for an aged Mariana sediment melt (open square with vertical cross) and assumed MORB sources (open, grey left pointing triangles). Various mixing curves between a single MORB source composition (open, left facing triangle) and the sedimentary compositions are shown. Tick marks are for the same weight fractions of the sedimentary material added on each curve and are labeled on curve A. The ($^{230}Th/^{232}Th$) for MORB sources are calculated from measured Th/U of erupted MORB, assuming that their source had been in secular equilibrium. This therefore implicitly assumes ^{238}U-^{230}Th disequilibrium in MORB is produced solely by ^{230}Th ingrowth during melting [e.g., *McKenzie*, 1985]. The MORB end-member of the mixing curves was chosen with ($^{230}Th/^{232}Th$) and $^{143}Nd/^{144}Nd$ at high and low ends of MORB field, respectively, to illustrate that even in this most favorable scenario, the mixing curve with bulk sediment does not pass through any part of the Mariana lava array. The dashed curve (C) shows mixing with an N-MORB source, with Th and Nd (also Nb and Ta, see below) elemental abundances taken from the N-MORB composition of *Sun and McDonough* [1989], assuming it represents a 10% melt. The solid curves represent mixing with a depleted MORB, calculated by fractional melting of the N-MORB source. The melting is designed to replicate a suitable high Ta/Nb subarc source. A melting model with 1% residual porosity, and melting to 5%, as is thought reasonable for backarc spreading [*Klein and Langmuir*, 1987], is used with the following bulk partition coefficients for initial (D) and melting modes (P) [*Shaw*, 1970]: $D_{Th} = 2.4x10^{-3}$, $D_{Nb} = 3.1x10^{-3}$, $D_{Ta} = 7.6x10^{-3}$, $D_{Nd} = 2.9x10^{-2}$ and $P_{Th} = 1.7x10^{-3}$, $P_{Nb} = 1.7x10^{-2}$, $D_{Ta} = 2.7x10^{-2}$, $D_{Nd} = 9.4x10^{-2}$ [after *Green et al.*, 1989; *Forsythe et al.*, 1994; *Hauri et al.*, 1994; *Lundstrom et al.*, 1994]. These values assume melting in the spinel stability field and yield a depleted mantle source with Ta/Nb of 0.15, which is close to a value obtained by extrapolation of the trend in Figure 7b back to appropriately low Th/Nb values. As is reasonable for melt depletion in the spinel stability field, the depleted MORB source is taken to have the same Th/U as the N-MORB source (and so plots in the same position in the diagram). The bulk sediment composition is taken from Table 2, assuming it is in secular equilibrium. The sediment melt is chosen with a ($^{230}Th/^{232}Th$) similar to the Uracas lavas, such that the mixing curve with depleted MORB passes through the bottom of the Mariana lava array and so serves to illustrate the required composition of the sedimentary component. The Th and Nd contents of the sediment melt are also somewhat arbitrarily calculated to be 13 and 50 ppm, respectively, from a model that produces a self-consistent sedimentary component within the somewhat uncertain constraints of sediment melt partitioning. (b) An equiline plot schematically showing the melting and aging processes required to produce a suitable enriched end-member component for the Mariana array from the bulk Mariana sediment composition. Symbols as in Figure 13a.

growth after U rich fluid addition, as in Figure 12b. Attempts to try to explain the full ($^{230}Th/^{232}Th$) variation in the Mariana lavas by variable sediment mixing alone (which corresponds to the scenario illustrated in Figure 12c), are not entirely successful (e.g., curve C, Figure 13a). Moreover, curve C requires a much less depleted mantle source, which is unlikely from the HSFE ratio considerations. These details aside, the sediment end-member nevertheless requires a much higher ($^{230}Th/^{232}Th$) than the bulk-subducted sediment (Figure 13a).

As argued above, it is not bulk sediment, but most probably a sediment melt that is variably added to the subarc mantle, and the sediment melting process may fractionate its Th/U. If the Th/U fractionation in the added sedimentary material occurred sufficiently long ago, this will also be reflected in the ($^{230}Th/^{232}Th$), as is shown in Figure 13b. This then is a straightforward way to account for the U-Th systematics of the Mariana lavas, that is also consistent with the other incompatible element data. It implies that addition of a fractionated sedimentary component to the subarc mantle occurred at least 350 kyr prior to fluid addition. This is only a minimum constraint, as after ~350 ka any ^{238}U-^{230}Th disequilibrium has decayed, and the chronometer has no further resolving power.

The time delay inferred between sediment fractionation and fluid addition helps rule out shallow contamination as an important source of incompatible elements in the Mariana lavas. If addition of a fractionated sediment component occurs by assimilation of crustal sediment melts, then the erupted lavas would retain the low ($^{230}Th/^{232}Th$) of the sedimentary source. Long crustal residence times would not make this hypothesis any more tenable, as not only are high ($^{230}Th/^{232}Th$) required by all the lavas, but many also have ^{238}U excesses, which would be destroyed by protracted evolution in a magma chamber.

Geochemical Constraints on the Structure and Dynamics of the Mariana Subduction Zone

There are some key features of the geochemical systematics of the Mariana lavas that place important constraints on possible physical models of the subduction zone. Two slab components are required, and the preservation of coherent element variations in the lavas suggests that there are only two dominant slab contributions. The slab components are most probably a sediment melt and an aqueous fluid derived from the altered oceanic crust. These fluxes must retain their discrete chemical signatures until they are brought together, in the source of the arc lava, very shortly before melting. Fitting all these considerations into a model that contains independent constraints from experimental petrology and geophysical modeling is not easy.

To illustrate some of the issues at stake, we discuss some simple arc models that attempt to address the geochemical observations. One other factor that we have felt is important to incorporate into the models is a mechanism to account for the ubiquitous occurrence of volcanic arc fronts 120 km above the Benioff zone [*Issacks and Barazangi*, 1977]. As has been proposed by previous work, we attribute this to a pressure sensitive dehydration reaction at this depth [*Green*, 1973] that releases water to trigger extensive mantle melting [*Tatsumi*, 1989]. There is not the space in this paper to discuss all the ramifications of suggested models for the many potential processes at work in the subarc mantle. We simply try to highlight what we consider some of the more important considerations.

Perhaps the simplest model calls on melting of the subducted sediment shallower than 120 km. Siliceous melts move into the overlying mantle and react to hybridize it [e.g., *Schiano et al.*, 1995], creating a sediment-enriched subarc mantle source that is dragged further downward with the subducting slab (Figure 14a). As the enriched mantle is downdragged, ^{238}U-^{230}Th disequilibrium created by addition of the sediment melt decays. A dehydration reaction in the altered oceanic crust releases the second slab component into the overlying enriched mantle and triggers extensive mantle melting (Figure 14a).

Although successful in keeping sediment and altered oceanic crust component separate and satisfying the constraints on the inferred timing of their additions, this model has several troublesome caveats. Recent thermal models [*Peacock*, 1991; *Davies and Stevenson*, 1992] would suggest that the surfaces of most (>20 Ma) slabs do not become hot enough for pelagic clays to melt [*Johnson and Plank*, 1993; *Nichols et al.*, 1994]. Nevertheless, modeling of the pressure, temperature, time (PTt) paths of descending slabs is highly dependent on the rather poorly known parameter of shear heating [*Peacock*, 1991; *Davies and Stevenson*, 1992], and more work is also required to define solidii for a range sediment compositions at high pressures [*Johnson and Plank*, 1993; *Nichols et al.*, 1994]. Given these uncertainties, the difference between some preferred slab PTt paths and the solidus of wet pelagic clay is not great (~50°C) [*Nichols et al.*, 1994].

Another problem with this model is that there is not a readily apparent dehydration reaction that might occur at 120 km depth (~30 kbar) in the altered oceanic crust. In a basaltic matrix, amphibole starts to dehydrate from some 80 km depth [*Hill and Boettcher*, 1970; *Lambert and Wyllie*, 1972]. This led *Tatsumi* [1989] to suggest that water derived from dehydration of the subducted crust reacts with the overlying mantle, which after being downdragged, itself dehydrates at 120 km [*Green*, 1973], triggering extensive mantle melting. This mechanism is not readily applicable to the model in Figure 14a as this would require aqueous fluid and sediment components to be downdragged together in the overlying mantle. During this time, radioactive decay would destroy the antithetic relationship between ^{238}U excesses and indices of sediment addition such as Th/Nb (Figure 5a). However, recent work of *Pawley and Holloway* [1993] and *Poli and Schmidt* [1995] shows that water can be carried farther than 80 km into the subduction zone by the basaltic oceanic crust, and for certain slab pressure-temperature trajectories, the altered oceanic crust may have a distinct pulse of fluid release at 100-120 km depth due to the zoisite/clinozoisite breakdown reaction [*Poli and Schmidt*, 1995]. This reaction is only applicable to hot slabs, in keeping with our requirement of sediment melting.

Our model 2 presents an alternative way to keep sediment and aqueous fluid fluxes separate until shortly before mantle melting (Figure 14b). The order of sediment and fluid addition to the subarc mantle is reversed. Dehydration of the slab produces at an overlying hydrated peridotite that is downdragged to 120 km where the mantle assemblage itself dehydrates to produce a LILE-rich fluid with large ^{238}U excesses that causes extensive melting, as in the model of *Tatsumi* [1989]. The sediment does not melt until much deeper in the mantle, but either focused fluid flow [*Spiegelman and McKenzie*, 1987] or buoyant upwelling of hybridized mantle brings sedimentary mate-

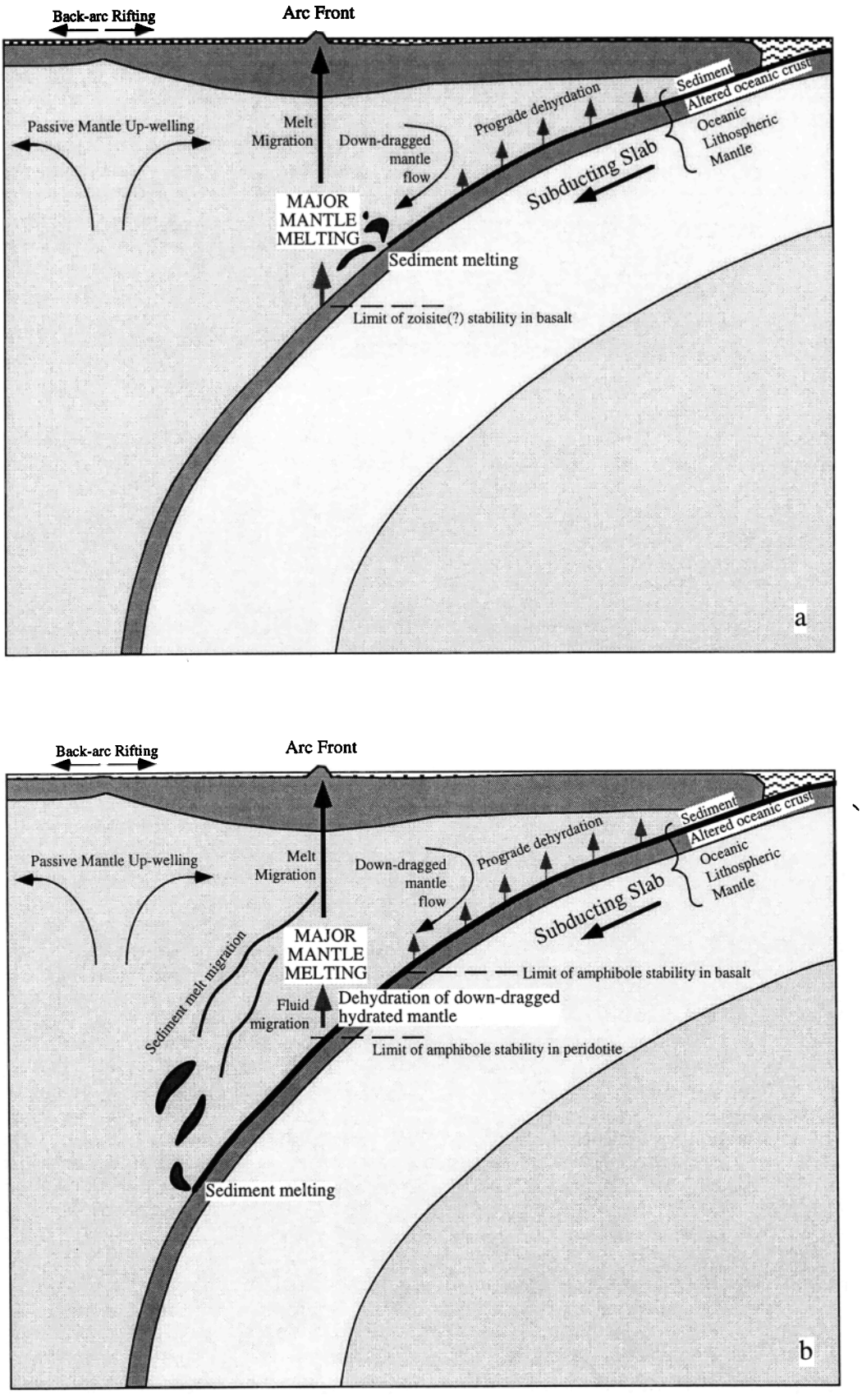

Figure 14. Cartoon of two possible physical models, discussed in the text, that can account for the key geochemical features observed in the Mariana lavas.

rial back into the subarc mantle through which the dehydration-triggered melts pass. In this manner, melts carrying an aqueous fluid signature variably interact with overlying material enriched by sediment melts. The movement from depth of sediment melts or sediment-enriched mantle into the zone of major mantle melting also gives time for any ^{238}U-^{230}Th disequilibrium produced during sediment melting to return to equilibrium.

Although perhaps less intuitive, model 2 is nonetheless not physically unreasonable. Of course, there are some troublesome aspects of this model, too. For example, the fluid released from the altered oceanic crust must pass through the overlying sediment without inheriting a significant sedimentary signature. However, prior to major basaltic dehydration, the sediments are likely to have themselves dehydrated and lost their inventory of most fluid mobile elements [*You et al.*, 1996]. The shallow mantle enriched by these sediment-derived fluids may not be entrained into the main downward flow in the mantle but may form serpentine diapirs which intrude forearcs [*Fryer*, 1992].

Comparison With Other Arcs

The Mariana arc is a classic intraoceanic subduction zone, and it has already been noted that the Mariana ^{238}U-^{230}Th and LILE/HSFE systematics resemble those observed globally. Likewise, ^{238}U-^{230}Th disequilibrium studies of other individual arcs have also noted multistage addition of slab components to the subarc mantle [*McDermott et al.*, 1993; *Reagan et al.*, 1994]. However, the relationship between ^{238}U-^{230}Th disequilibrium and other key geochemical indices differs in detail for the few existing studies that include such data. For example, in Chile, ^{238}U excesses correlate with $^{10}Be/^{9}Be$ (an index of sediment addition) [*Sigmarsson et al.*, 1990], in Nicaragua and the Bismarck arcs $^{10}Be/^{9}Be$ correlates with ($^{230}Th/^{232}Th$) but not the modest degrees of disequilibrium [*Reagan et al.*, 1994; *Gill et al.*, 1993], while in the Marianas and also the Lesser Antilles [*Turner et al.*, 1996], ^{238}U excesses correlate inversely with indices of sediment addition. This range of behavior can be reasonably explained by variations in the composition of subducted sediment and the timing of slab addition events.

Both this work and that of *Sigmarsson et al.* [1990] and *Reagan et al.* [1994], suggest that the added sedimentary component preferentially carries U relative to Th and hence ^{238}U excesses (e.g., Figure 13b). If the subarc mantle melts soon after such sediment addition, correlations between indices of sediment addition with ^{238}U excesses would be expected, as is observed at Chile [*Sigmarsson et al.*, 1990]. In the Marianas, however, it is argued that sufficient time elapses such that any disequilibrium produced by addition of the sediment melt has decayed by the time of aqueous fluid addition and major mantle melting. The inferred difference of timing of sediment addition at the Marianas and Chile may reflect the very different physical subduction parameters of the two arcs [*Jarrard*, 1986].

The difference between the systematics of Nicaragua/Bismarck arcs and Mariana/Lesser Antilles may be largely rooted in the composition of the added sediment. Quantitative calculations are not possible as the requisite Th and U data are not available for subducting sediment from all localities, but gross differences are known that provide a conceptual model. Outboard of Guatemala (DSDP Site 495), and perhaps all of Central America, carbonate-rich sediments and organic-rich hemipelagic muds have high U contents, very high U/Th, and thus high ($^{230}Th/^{232}Th$) even compared to MORB [*Reagan et al.*, 1994; M. Carr, personal communication, 1996]. Although the Bismarck sediments have never been drilled, the extremely high ($^{230}Th/^{232}Th$) of the lavas implies subduction of similarly high U/Th sediments. Mixing of U-rich sediments with ($^{230}Th/^{232}Th$)~6 [*Reagan et al.*, 1994] and a MORB-like subarc mantle, ($^{230}Th/^{232}Th$) ~1-1.5, can create a large range of ($^{230}Th/^{232}Th$). Since the added sediments have high U content, the subsequent effect of aqueous fluid addition on the total U budget will be small, and hence ^{238}U excesses will be small even in the comparatively sediment poor sources. Thus the effect of adding variable amounts of U-rich carbonate sediment to the Nicaraguan source results in large variations in ($^{230}Th/^{232}Th$) but small variations in ^{238}U excesses. This contrasts with the systematics resulting from the comparatively Th-rich sediment addition at the Marianas. There clearly may be additional thermal or tectonic factors, but to a first order, differences in sediment input appear to account for the rather different U-Th systematics of Nicaraguan and Mariana lavas.

One further issue that perhaps needs to be raised is B and Be systematics. The two-component model inferred from this and other studies appears to conflict with the cogent arguments for a single slab flux presented by *Morris et al.* [1990] from B-Be analyses. *Morris et al.* [1990] require a slab-derived end-member that carries ^{10}Be from the sediment but has B/Be higher than bulk sediment. They inferred that this subduction component was a mixture of both sediment and aqueous fluid from the altered oceanic crust, the latter raising the overall B/Be. Since arrays of lavas from several arcs appear to have zero intercepts on plots of $^{10}Be/^{9}Be$ versus B/Be, *Morris et al.* [1990] inferred that the mantle source to which the subduction zone component was added was itself free of B-enriched slab components.

We would interpret the high $^{10}Be/^{9}Be$ end-member to represent a sediment melt which is likely to have elevated B/Be with respect to bulk sediment due to melt fractionation, without additionally requiring a contribution from the altered oceanic crust. That the array from sediment-rich to sediment-poor lavas is not rotated by subsequent fluid addition away from a zero intercept on the $^{10}Be/^{9}Be$ versus B/Be plot has several possible explanations. For the arcs studied by *Morris et al.* [1990], the subsequent fluid addition may have been minor compared to the Marianas. Alternatively, B may be almost completely lost at shallow levels in the subduction zone [*Moran et al.*, 1992; *Bebout et al.*, 1993; *Ryan et al.*, 1993; *You et al.*, 1996], and so addition of aqueous fluids to the mantle wedge deeper in the subduction zone may be able to significantly affect ratios such as Ba/Nb, Pb/Ce without greatly changing B/Be. These hypotheses clearly need to be tested by analyzing the different sample suites for the same tracers.

Conclusions

Beneath the Mariana arc, most elements are transferred from the subducted slab to the subarc mantle by two discrete processes. Subducted sediment material is transported into the mantle wedge as a fluid phase, which from geochemical constraints is most likely to be a melt. This inferred melting process fractionates some elements relative to the bulk-subducted sediment. For example, Nb is strongly fractionated from La

and Th by residual rutile. The main differences in the composition of erupted lavas from different islands of the Marianas are due to variable amounts of the sediment melt addition to their sources. Second-order chemical variation in erupted lavas may result from variability in the subducted assemblage due to the heterogeneous distribution of the Magellan seamounts on the subducting plate.

At least 350 kyr after the addition of sedimentary material, a dehydration event in the slab releases an aqueous fluid which preferentially carries an additional flux of elements (especially Ba and Pb) into the mantle wedge. Signatures of the aqueous fluid addition are inversely correlated with indices of sediment melt contribution. This relationship is only expected if there is a fairly constant aqueous fluid flux across the whole arc. The aqueous fluid flux is most likely derived from the altered oceanic crust and produces large ^{238}U excesses in the mantle wedge and ultimately the erupted lavas. The near horizontal array of Mariana lavas on the equiline diagram consequently implies that aqueous fluid addition, melting and eruption of magma occurs in <30 kyr. This suggests very rapid melt migration and that the aqueous fluid flux may trigger major mantle melting. The unmodified Mariana subarc mantle is highly depleted, presumably due to prior backarc melt extraction.

Subducted sediments and aqueous fluids have been long been implicated in the chemistry of volcanic arcs. Many earlier subduction zone models have invoked two slab-derived components [*Kay*, 1980; *Ellam and Hawkesworth*, 1988; *McDermott et al.*, 1993; *Miller et al.*, 1994; *Reagan et al.*, 1994] and some have even specifically related these phases to sediment melting and basalt dehydration [*Plank and Langmuir*, 1992; *Plank*, 1993; *Miller*, 1995; *Turner et al.*, 1996]. However, we feel the combination of tracers used in this study both strengthens earlier inferences and enables a timing of these events to be derived. More high-quality geochemical data sets for other arc systems, and additional high-pressure fluids and melt-partitioning experiments will help further resolve these processes and determine if they are common to all arc systems.

Appendix: Analytical Techniques

All samples were crushed in agate. Major elements and some trace elements of the Mariana volcanics were measured by XRF at the University of Massachusetts using techniques reported by *Rhodes* [1983]. A greater range of trace elements concentrations were determined by ICP-MS at Cornell, which enabled the analysis of elements found at very low abundances in arcs lavas and for which existing data are sparse and often of poor precision. Procedures were similar to those reported by *Cheatham et al.* [1992], except that perchloric acid was excluded from the digestion mix to avoid interferences on the LREE [*Longerich*, 1993]. Special attention was paid to the high field strength elements (Zr, Hf, Nb, and Ta). No problems of solution instability nor incomplete dissolution were encountered, and solutions rerun after several months gave statistically identical results. USGS standards BIR, DNC, and W2 were used for external calibration of high field strength elements, following independent determinations based on the method of standard additions (for Nb and Ta) and isotope dilution (for Zr and Hf). Values used are shown in Table A1. Table 1 indicates values obtained for JA-1, analyzed as an unknown with the Marianas samples. Further details on the ICP-MS procedures are available from T. Plank on request. There is excellent agreement between ICP-MS and XRF Zr, Ba, and Sr (with mean relative differences of 4%, 2%, and 7%, respectively; most of the differences are due to slightly different standard values used in the calibrations), between ICP-MS and perchloric acid dissolution, isotope dilution sector mass spectrometric U and Th determinations (mean relative differences better than 2 and 3%) (see Figure A1), and also ICP-MS and INAA [*Potts et al.*, 1985] Ta measurements (better than 8%, which is close to the precision of INAA at the low Ta concentrations of the samples measured).

Isotopic composition measurements of Sr, Nd, and Pb were made at the Vrije Universiteit, Amsterdam, using standard chemical techniques and a Finnigan MAT 261 mass spectrometer with nine fixed Faraday collectors. Sr isotope ratios were measured dynamically and linearly fractionation corrected to $^{86}Sr/^{88}Sr=0.1194$. Nd was measured dynamically as Nd^+ and exponentially fractionation corrected to $^{144}Nd/^{146}Nd=0.7219$. The mean values obtained during the period of this study for NBS 987 and the La Jolla Nd standard were $^{87}Sr/^{86}Sr=0.710286$ and $^{143}Nd/^{144}Nd=0.511848$, respectively. Pb isotope measurements were made statically, and samples were corrected for mass fractionation using a coefficient obtained from the mean values of NBS 981 obtained during this study, $^{206}Pb/^{204}Pb=16.891$, $^{207}Pb/^{204}Pb=15.423$ and $^{208}Pb/^{204}Pb=36.492$, relative to the values of [*Todt et al.*, 1984]. Two sigma standard deviations of repeat measurements (hereafter termed reproducibility) of Sr, Nd, and Pb standards for the period of measurement were 0.0028% (n=8), 0.0022% (n=5), and 0.026%/amu (n=9) respectively. Since the Nd iso-

Table A1. Elemental Abundances Used for the Three Standards Run to Calibrate ICP-MS During Measurement of Mariana Samples

	Rb	Sr	Y	Zr	Nb	Cs	Ba		Hf	Ta	Pb	Th	U
BIR	0.23	111	15.5	15.2	0.546	0.004	6.63		0.596	0.045	2.88	0.031	0.0085
DNC	3.9	144.5	17.7	36.9	1.47	0.207	103.3		0.995	0.095	6.2	0.24	0.05
W2	21	197	21.9	93.1	7.7	0.902	171.6		2.48	0.5	7.7	2.1	0.49
	La	Ce	Pr	Nd	Sm	Eu	Gd	Tb	Dy	Ho	Er	Yb	Lu
BIR	0.56	1.9	0.39	2.4	1.11	0.52	1.98	0.41	2.62	0.59	1.71	1.7	0.26
DNC	3.56	8.11	1.12	4.98	1.43	0.57	2.11	0.43	2.76	0.62	1.87	1.97	0.32
W2	10.07	22.79	3.04	12.9	3.24	1.1	3.73	0.68	3.83	0.8	2.17	1.98	0.3

In units of μg/g.

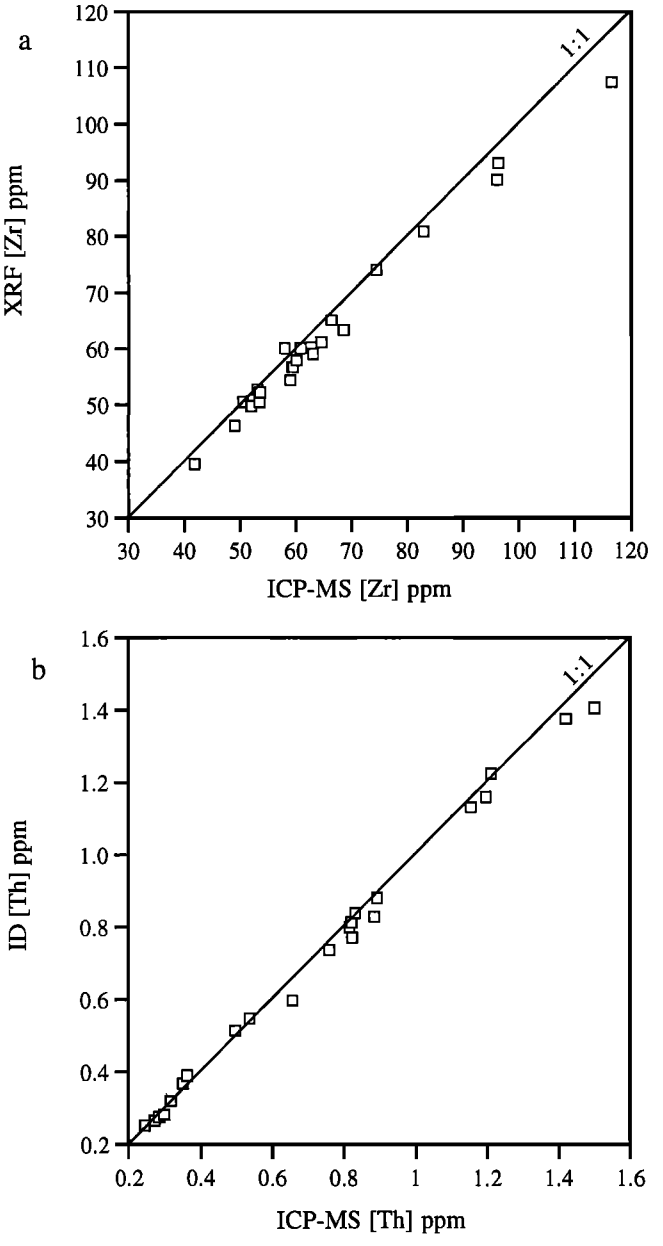

Figure A1. Comparison of selected elemental concentrations of the Mariana volcanics (open squares) obtained by different analytical techniques. (a) ICP-MS versus X ray fluorescence (XRF) Zr concentration data and (b) ICP-MS versus isotope dilution, secondary-ionization mass spectrometry (ID-SIMS) Th concentration data. Variability between duplicate sample pellets (XRF), repeat runs of the same dissolution (ICP-MS), or repeat measurements (ID-SIMS) is smaller than the symbol size in all but a very few instances.

topic variations are rather small, six samples were measured in duplicate (starting with different dissolutions). All duplicate measurements were within the reproducibility gauged from replicate standard measurements. Sr isotopic analysis were made from powders that had first been leached by 1 N HCl for 30 min in an ultrasound bath to ensure removal of any sea spray contamination that has been found to affect some oceanic island samples [e.g., *Hemond et al.*, 1993]. Blanks for Sr, Nd, and Pb are typically 100, 20, and 200 pg, respectively.

Th and U isotopic concentration measurements were made at Lamont-Doherty Earth Observatory on the Isolab 54 using techniques reported by *England et al.* [1992] and A. Zindler et al. (Measurement of $^{230}Th/^{232}Th$ in volcanic rocks using secondary ion mass spectrometry, submitted to Analytical Chemistry, 1996). Briefly, samples were spiked with a ^{233}U-^{229}Th spike and dissolved in a HF-$HClO_4$-HCl-HNO_3 mix. Elemental concentrations were determined by isotope dilution on the same runs as isotopic ratio measurements. U was loaded with colloidal graphite on single rhenium filaments and run thermally using a routine that switched the $^{238}U^+$ beam between three axial faraday collectors so that in turn $^{233}U^+$, $^{234}U^+$, and $^{235}U^+$ could be simultaneously measured on a Daly collector lying behind an electrostatic energy filter. Measurements were fractionation corrected to a $^{238}U/^{235}U$ of 137.88. The reproducibility of an internal U standard with $^{233}U/^{238}U$ 6.08×10^{-5} was 0.8% and the ($^{234}U/^{238}U$) of all samples measured was 1.00 but with a slightly poorer reproducibility of 1.3%. Duplicate measurement of ASC 3 reproduced U concentrations to much better than 0.5%. Th was loaded together with some colloidal graphite onto a small platform machined onto a pyrolized graphite rod, and then ionized with a 15 kV Ar^+ ion beam. This technique yields very high Th ionization efficiencies (>0.5%). The $^{232}Th^+$ beams were switched between two axial faraday cups to enable simultaneous measurement of $^{230}Th^+$ and $^{229}Th^+$ in turn on the Daly. Within-run counting statistics (2σ standard error) for the $^{230}Th/^{232}Th$ ratio were generally between 1 and 0.5% and reproducibility determined by triplicate measurement of ASC 3 and an in-house standard ($^{230}Th/^{232}Th = 6.45 \times 10^{-6}$) are better than 1%. Atomic ratios are converted into activity ratios using the compilation of activity coefficients used by *Goldstein et al.* [1989]; namely, $\lambda(^{238}U) = 1.551 \times 10^{-10}$ yr^{-1}, $\lambda(^{234}U) = 2.835 \times 10^{-6}$ yr^{-1}, $\lambda(^{232}Th) = 4.948 \times 10^{-11}$ yr^{-1} and $\lambda(^{230}Th) = 9.195 \times 10^{-6}$ yr.$^{-1}$

Acknowledgments. We are greatly indebted to John Beavan for his work in organizing the PSP 93 GPS campaign and giving free reign to T.E. during the expedition to the Marianas. We would also like to thank the Government of the Northern Marianas for cooperation and assistance. The efforts of Captain and crew of M/V *Celeste* are much appreciated, which, together with the help and good company provided by the Saipan team and other members of PSP 93, made sample collection a most enjoyable task. Mike Rhodes and all at the Raymond B. Gilmore XRF facility provided great analyses and hospitality. Thanks to Jon Woodhead for samples and good advice at the inception of this project. Dick Moore provided important additional samples and much useful information. Nick Rogers kindly ran some INAA cross checks. Discussions with many people at Lamont, in particular, Charlie Langmuir, Ro Kinzler, and Krikitt Johnson helped shape ideas. T.E. is grateful for guidance on many key matters from Jim Rubenstone, Vincent Salters, Afi Saachi-Kocher, and Louis Falbourne. Thanks also to Arnd Heumann for ever timely computer advice. We much appreciated the thorough formal reviews by Jon Davidson and Bob Stern, the editorial work of Marc Defant and Steven L. Goldstein, and comments from Gareth Davies, David Hilton, and Mark Reagan which significantly improved the manuscript. T.P. gratefully acknowledges Michael Cheatham for training and advice in the ICP-MS analyses and an NSF Postdoctoral Fellowship (EAR-9203151) for support. Financial support to T.E. from a NATO postdoctoral fellowship (GT8/F/91/GS/1) and the Vrije Universiteit; A.Z., W.W., and B.B. from NSF. This is NSG contribution 970129

References

Abrams, L.J., R.L. Larson, T.H. Shipley, and Y. Lancelot, The seismic stratigraphy and sedimentary history of the East Mariana and

Pigafetta basins of the western Pacific, *Proc. Ocean Drill. Program, Sci. Results, 129*, 551-569, 1992.

Arculus, R.J., and R. Powell, Source component mixing in the regions of arc magma generation, *J. Geophys. Res., 91*, 5913-5926, 1986.

Ayers, J.C., and D.H. Eggler, Partitioning of elements between silicate melt and H_2O-NaCl fluids at 1.5 and 2.0GPa pressure: Implications for mantle metasomatism, *Geochim. Cosmochim. Acta, 59*, 4237-4246, 1995.

Ballhaus, C., R.F. Berry, and D.H. Green, Oxygen fugacity controls in the Earth's upper mantle, *Nature, 348*, 437-440, 1990.

Beattie, P.D., The generation of uranium series disequilibrium by partial melting of spinel peridotite: Constraints from partitioning studies, *Earth Planet. Sci. Lett., 117*, 379-391, 1993.

Bebout, G.E., J.G. Ryan, and W.P. Leeman, B-Be systematics in subduction-related metamorphic rocks: Characterisation of the subducted component, *Geochim. Cosmochim. Acta, 57*, 2227-2237, 1993.

Ben Othman, D., W.M. White, and J. Patchett, The geochemistry of marine sediments, island arc magma genesis, and crust-mantle recycling, *Earth Planet. Sci. Lett., 94*, 1-21, 1989.

Bloomer, S.H., R.J. Stern, and N.C. Smoot, Physical volcanology of the submarine Mariana and Volcano arcs, *Bull. Volcanol., 51*, 210-224, 1989.

Brenan, J.M., H.F. Shaw, D.L. Phinney, and J.F. Ryerson, Rutile-aqueous fluid partitioning of Nb, Ta, Hf, Zr, U, and Th: Implications for high field strength element depletions in island arc basalts, *Earth Planet. Sci. Lett., 128*, 327-339, 1994.

Brenan, J., H.F. Shaw, F.J. Ryerson, and D.L. Phinney, Mineral-aqueous fluid partitioning of trace elements at 900°C and 2.0GPa: Constraints on the trace element chemistry of mantle and deep crustal fluids, *Geochim. Cosmochim. Acta, 59*, 3331-3350, 1995a.

Brenan, J.M., H.F. Shaw, and F.J. Ryerson, Experimental evidence for the origin of lead enrichment in convergent-margin magmas, *Nature, 378*, 54-56, 1995b.

Cheatham, M.M., W.F. Sangrey, and W.M. White, Improved ICP-MS analytical precision using non-linear response drift corrections, in *Winter Conference on Plasma Spectrochemistry*, edited by R. Barnes, Univ. of Mass., Amherst, 1992.

Chow, T.J., R.J. Stern, and T.H. Dixon, Absolute and relative abundances of K, Rb, Sr and Ba in circum-Pacific island-arc magmas, with special reference to the Marianas, *Chem. Geol., 28*, 111-121, 1980.

Condomines, M., and O. Sigmarsson, Why are so many arc magmas close to ^{238}U-^{230}Th radioactive equilibrium?, *Geochim. Cosmochim. Acta, 57*, 4491-4497, 1993.

Davidson, J.P., Crustal contamination vs. subduction zone enrichment: Examples from the Lesser Antilles and implications for mantle source compositions of island arc volcanic rocks, *Geochim. Cosmochim. Acta, 51*, 2185-2198, 1987.

Davies, J.H., and D.J. Stevenson, Physical model of source region of subduction zone volcanics, *J. Geophys. Res., 97*, 2037-2070, 1992.

Dixon, T.H., and R. Batiza, Petrology and chemistry of recent lavas in the northern Marianas: Implications for the origin of island arc basalts, *Contrib. Mineral Petrol., 70*, 167-181, 1979.

Dixon, T.H., and R.J. Stern, Petrology, chemistry and isotopic composition of submarine volcanoes in the southern Mariana arc, *Geol. Soc. Am. Bull., 94*, 1159-1172, 1983.

Dosso, L., H. Bougault, and J.-L. Joron, Geochemical morphology of the north Mid-Atlantic ridge, 10-24°N: Trace element-isotope complementarity, *Earth Planet. Sci. Lett., 120*, 443-462, 1993.

Elderfield, H., C.J. Hawkesworth, M J Greaves, and S.E. Calvert, Rare earth element geochemistry of oceanic ferromanganese nodules and associated sediment, *Geochim. Cosmochim Acta, 45*, 513-528, 1981.

Ellam, R.M., and C.J. Hawkesworth, Elemental and isotopic variations in subduction related basalts: Evidence for a three component model, *Contrib. Mineral. Petrol., 98*, 72-80, 1988.

England, J.G., et al., The Lamont-Doherty Geological Observatory Isolab 54 isotope ratio mass spectrometer, *Int. J. Mass Spectrom. Ion Processes, 121*, 201-240, 1992.

Forsythe, L.M., R.L. Nielsen, and M.R. Fisk, High-field strength element partitioning between pyroxene and basaltic to dacitic magmas, *Chem. Geol., 117*, 107-125, 1994.

Fryer, P., A synthesis of Leg 125 drilling of serpentinite seamounts on the Mariana and Izu-Bonin forearcs, *Proc. Ocean Drill. Program, Sci. Results, 125*, 593-614, 1992.

Fryer, P., and D.H. Hussong, Seafloor spreading in the Mariana Trough: Results of Leg 60 drilling site selection surveys, *Initial Rep. Deep Sea Drill. Proj., 60*, 45-55, 1981.

Gill, J.B., *Orogenic Andesites and Plate Tectonics*, 330 pp., Springer-Verlag, New York, 1981.

Gill, J.B., and R.W. Williams, Th isotope and U-series studies of subduction-related volcanic rocks, *Geochim. Cosmochim. Acta, 54*, 1427-1442, 1990.

Gill, J.B., J.D. Morris, and R.W. Johnson, Timescales for producing the geochemical signature of island arc magmas: U-Th-Po and Be-B systematics in recent Papua New Guinea lavas, *Geochim. Cosmochim Acta, 57*, 4269-4283, 1993.

Goldstein, S.J., M.T. Murrel, and D.R. Janecky, Th and U isotopic systematics of basalts from the Juan de Fuca and Gorda Ridges by mass spectrometry, *Earth Planet. Sci. Lett., 96*, 134-146, 1989.

Green, D.H., Experimental melting studies on a model upper mantle composition at high pressure under water-saturated and water-undersaturated conditions, *Earth Planet. Sci. Lett., 19*, 37-53, 1973.

Green, T.H., Experimental studies of trace-element partitioning applicable to igneous petrogenesis-Sedona 16 years later, *Chem. Geol., 117*, 1-36, 1994.

Green, T.H., and N.J. Pearson, An experimental study of Nb and Ta partitioning between Ti-rich minerals and silicate liquids at high temperature and pressure, *Geochim. Cosmochim. Acta, 51*, 55-62, 1987.

Green, T.H., S.H. Sie, C.G. Ryan, and D.R. Cousens, Proton microprobe-determined partitioning of Nb, Ta, Zr, Sr and Y between garnet, clinopyroxene and basaltic magma at high pressure and temperature, *Chem. Geol., 74*, 201-216, 1989.

Hauri, E.K., T.P. Wagner, and T.L. Grove, Experimental and natural partitioning of Th, U, Pb and other trace elements between garnet, clinopyroxene and basaltic melts, *Chem. Geol., 117*, 149-166, 1994.

Hawkesworth, C.J , J.M. Hergt, R.M. Ellam, and F. McDermott, Element fluxes associated with subduction related magmatism, *Philos. Trans. R. Soc. London, Ser. A, 335*, 393-405, 1991.

Hawkesworth, C.J., K. Gallagher, J.M. Hergt, and F. McDermott, Mantle and slab contributions in arc magmas, *Annu. Rev. Earth Planet. Sci., 21*, 175-204, 1993a.

Hawkesworth, C.J., K. Gallagher, J.M. Hergt, and F. McDermott, Trace element fractionation processes in the generation of island arc basalts, *Philos. Trans. R. Soc. London, Ser. A, 342*, 179-191, 1993b.

Hemond, C., N.T. Arndt, U. Lichtenstein, and A. Hofmann, The heterogeneous Iceland plume: Nd-Sr-O Isotopes and trace element constraints, *J. Geophys. Res., 98*, 16833-15850, 1993.

Hildreth, W., and S. Moorbath, Crustal contributions to arc magmatism in the Andes of central Chile, *Contrib. Mineral. Petrol., 98*, 455-489, 1988.

Hill, R.T.E., and A.L. Boettcher, Water in the Earth's mantle: Melting curves of basalt-water and basalt-water-carbon dioxide, *Science, 167*, 980-982, 1970.

Hofmann, A.W., Chemical differentiation of the Earth: The relationship between mantle, continental crust, and oceanic crust, *Earth Planet. Sci. Lett., 90*, 297-314, 1988.

Hofmann, A.W., K.P. Jochum, M. Seufert, and W.M. White, Nb and Pb in oceanic basalts: New constraints on mantle evolution, *Earth Planet. Sci. Lett., 79*, 33-45, 1986.

Hole, M.J., A.D. Saunders, G.F. Marriner, and J. Tarney, Subduction of pelagic sediments: Implications for the origin of Ce-anomalous basalts from the Mariana Islands, *J. Geol. Soc. London, 141*, 453-472, 1984.

Irifune, T., A.E. Ringwood, and W.O. Hibberson, Subduction of continental crust and terrigenous and pelagic sediments: An experimental study, *Earth Planet. Sci. Lett., 126*, 351-368, 1994.

Ishikawa, T., and E. Nakamura, Origin of the slab component in arc lavas from across-arc variation of B and Pb isotopes, *Nature, 370*, 205-208, 1994.

Issacks, B.L., and M. Barazangi, Geometry of Benioff Zones: Lateral segmentation and downwards bending of subducted lithosphere, in *Island Arcs, Deep Sea Trenches and Backarc Basin, Maurice Ewing Ser.*, vol. 1, edited by M. Talwani and W.C.Pitman III, pp. 99-114, AGU, Washington, D. C., 1977.

Ito, E., and R.J. Stern, Oxygen- and strontium-isotopic investigations of subduction zone volcanism: The case of the Volcano arc and the Mariana island arc, *Earth Planet. Sci. Lett., 76*, 312-320, 1985/1986.

Jarrard, R.D., Relations among subduction parameters, *Rev. Geophys., 24*, 217-284, 1986.

Jenner, G.A., S.F. Foley, S.E. Jackson, T.H. Green, B.J. Fryer, and H.P.

Longerich, Determination of partition coefficients for trace elements in high pressure-temperature experimental run products by laser ablation microprobe-inductively coupled plasma mass spectrometry (LAM-ICP-MS), *Geochim. Cosmochim. Acta, 57*, 5099-5103, 1993.

Jochum, J.P , A.W. Hofmann, E. Ito, H.M. Seufert, and W.M. White, K, U and Th in mid-oceanic ridge basalt glasses and heat production, K/U and K/Rb in the mantle, *Nature, 306*, 431-436, 1983.

Jochum, K.P., H.M. Seufert, B. Spettel, and H. Palme, The solar-system abundances of Nb, Ta and Y, and the relative abundances of refractory lithophile elements in differentiated planetary bodies, *Geochim. Cosmochim. Acta, 50*, 1173-1183, 1986.

Jochum, K.P., W.F. McDonough, H. Palme, and B. Spettel, Compositional constraints on the continental lithospheric mantle from trace elements in spinel peridotite xenoliths, *Nature, 340*, 548-550, 1989.

Johnson, K.T.M., H.J.B. Dick, and N. Shimizu, Melting in the oceanic upper mantle: an ion microprobe study of diopsides in abyssal peridotites, *J. Geophys. Res., 95*, 2661-2678, 1990.

Johnson, M.C., and T. Plank, Experimental constraints on sediment melting during subduction, *Eos Trans. AGU, 74 (43)*, Fall Meet. Suppl., 680, 1993.

Karl, S.M., G.A. Wandless, and A.M. Karpoff, Sedimentological and geochemical characteristics of Leg 129 siliceous deposits, *Proc. Ocean Drill. Program, Sci. Results, 129*, 31-80, 1992.

Karpoff, A.M., Cenezoic and Mesozoic sediments from the Pigafetta Basin, Leg 129, Sites 800 and 801: Mineralogical and geochemical trends of the deposits overlying the oldest oceanic crust, *Proc. Ocean Drill. Program, Sci. Results, 129*, 3-30, 1992.

Kay, R.W., Volcanic arc magmas: Implications of a melting-mixing model for element recycling in the crust-upper mantle system, *J. Geol., 88*, 497-522, 1980.

Kelemen, P.B., R.J. Kinzler, K.T.M Johnson, and A.J. Irving, High field strength element depletions in arc basalts due to magma-mantle interaction, *Nature, 345*, 521-524, 1990.

Kelemen, P.B., N. Shimizu, and T. Dunn, Relative depletion of niobium in some arc magmas and the continental crust: Partitioning of K, Nb, La and Ce during melt/rock reaction in the upper mantle, *Earth Planet. Sci. Lett., 120*, 111-134, 1993.

Keppler, H., Constraints from partitioning experiments on the composition of subduction-zone fluids, *Nature, 380*, 237-240, 1996.

Klein, E.M., and C.H. Langmuir, Global correlations of ocean ridge basalt chemistry and axial depth and crustal thickness, *J. Geophys. Res., 92*, 8089-8115, 1987.

Lambert, I.B., and P.J. Wyllie, Melting of gabbro (quartz eclogite) with excess water to 35 kilobars, with geological implications, *J. Geol., 80*, 693-708, 1972.

Lancelot, Y., et al., *Proceedings of the Ocean Drilling Program, Initial Reports*, vol. 129, 488 pp., Ocean Drill. Program, College Station, Tex., 1990.

Langmuir, C.H., E. Klein, and T. Plank, Petrological systematics of mid-oceanic ridge basalts: constraints on melt generation beneath ocean ridges, in *Mantle Flow and Melt Generation at Mid-ocean Ridges*, edited by J.P. Morgan, D.K. Blackman, and J.M. Sinton, pp. 183-280, AGU, Washington, D. C., 1992.

LaTourette, T.Z., and D.S. Burnett, Experimental determination of U and Th partitioning between clinopyroxene and natural and synthetic basaltic liquid, *Earth Planet. Sci. Lett., 110*, 227-244, 1992.

Lee, J., R.J. Stern, and S.H. Bloomer, Forty million years of magmatic evolution in the Mariana arc: The tephra glass record, *J. Geophys. Res., 100*, 17671-17687, 1995.

Lin, P.-N., Trace element and isotopic characteristics of western Pacific pelagic sediments: Implications for the petrogenesis of Mariana Arc magmas, *Geochim. Cosmochim. Acta, 56*, 1641-1654, 1992.

Lin, P.-N., R.J. Stern, and S.H. Bloomer, Shoshonitic volcanism in the northern Mariana arc, 2, Large-ion lithophile and rare earth element abundances: Evidence for the source of incompatible element enrichments in intraoceanic arcs, *J. Geophys. Res., 94*, 4497-4514, 1989.

Lin, P.N., R.J. Stern, J.D. Morris, and S.H. Bloomer, Nd- and Sr-isotopic compositions of lavas from the northern Mariana and southern Volcano arcs: Implications for the origin of island arc melts, *Contrib. Mineral. Petrol., 105*, 381-392, 1990.

Longerich, H.P., Oxychlorine ions in inductively coupled plasma mass spectrometry: Effect of chlorine speciation as Cl^- and ClO_4^-, *J. Anal. At. Spectrom., 8*, 439-444, 1993.

Lundstrom, C.C., H.F. Shaw, F.J. Ryerson, D.L. Phinney, J.B. Gill, and Q. Williams, Compositional controls on the partitioning of U, Th, Ba, Pb, Sr and Zr between clinopyroxene and haplobasaltic melts: Implications for uranium series disequilibria in basalts, *Earth Planet. Sci. Lett., 128*, 407-423, 1994.

Maury, R.C., M.J. Defant, and J.-L. Joron, Metasomatism of the subarc mantle inferred from trace element in Philippine xenoliths, *Nature, 360*, 661-663, 1992.

McCallum, I.S., and M.P. Charette, Zr and Nb partition coefficients: Implications for the genesis of mare basalts, KREEP and sea floor basalts, *Geochim. Cosmochim. Acta, 42*, 859-869, 1978.

McCulloch, M.T., and J.A. Gamble, Geochemical and geodynamical constraints on subduction zone magmatism, *Earth Planet. Sci. Lett., 102*, 358-374, 1991.

McDermott, F.M., and C. Hawkesworth, Th, Pb, and Sr isotope variations in young island arc volcanics and oceanic sediments, *Earth Planet. Sci . Lett., 104*, 1-15, 1991.

McDermott, F., M.J. Defant, C.J. Hawkesworth, R.C. Maury, and J.L. Joron, Isotopic and trace element evidence for three component mixing in the genesis of the North Luzon arc lavas, *Contrib. Mineral. Petrol., 113*, 9-23, 1993.

McKenzie, D., ^{230}Th-^{238}U disequilibrium and the melting process beneath ridge axes, *Earth Planet. Sci. Lett., 72*, 149-157, 1985.

Meijer, A., Pb and Sr isotopic data bearing on the origin of volcanic rocks from the Mariana island-arc system, *Geol. Soc. Am. Bull., 87*, 1358-1369, 1976.

Meijer, A., Mariana-Volcano Islands, in *Andesites*, edited by R.S. Thorpe, pp. 293-306, John Wiley, New York, 1982.

Meijer, A., and M. Reagan, Petrology and geochemistry of the island of Sarigan in the Mariana arc: Calc-alkaline volcanism in an oceanic setting, *Contrib. Mineral. Petrol., 77*, 337-354, 1981.

Meijer, A., and M. Reagan, Origin of K_2O-SiO_2 trends in volcanoes of the Marianas arc, *Geology, 11*, 67-71, 1983.

Meijer, A., M. Reagan, H. Ellis, M. Shafiqullah, J. Sutter, P. Damon, and S. Kling, Chronology of volcanic events in the eastern Philippine Sea, in *The Tectonic and Geologic Evolution of the Southeast Asian Seas and Islands: Part 2 Geophys. Monogr. Ser.*, vol. 27, edited by D.E. Hayes, pp. 349-359, AGU, Washington, D. C., 1983.

Miller, D.M., Petrogenesis of adjacent calc-alkaline and tholeiitic volcanoes on Umnak Island, Aleutian Islands, Alaska, *Ph.D. thesis*, 455 pp., Columbia Univ., New York, 1995.

Miller, D.M., S.L. Goldstein, and C.H. Langmuir, Cerium/lead and lead isotope ratios in arc magmas and the enrichment of lead in the continents, *Nature, 368*, 514-520, 1994.

Monaghan, M.C., J. Klein, and C.I. Measures, The origin of ^{10}Be in island arc volcanic rocks, *Earth Planet. Sci. Lett., 89*, 288-298, 1988.

Moran, A.E., V.B. Sisson, and W.P. Leeman, Boron depletion during progressive metamorphism: Implications for subduction processes, *Earth Planet. Sci. Lett., 111*, 331-349, 1992.

Morris, J., and F. Tera, $^{10}Be/^{9}Be$ in mineral separates and whole rocks from volcanic arcs: Implications for sediment subduction, *Geochim. Cosmochim. Acta, 53*, 3197-3206, 1989.

Morris, J., W.P. Leeman, and F. Tera, The subducted component in island arc lavas: Constraints from Be isotopes and B-Be systematics, *Nature, 344*, 31-36, 1990.

Morris, J.D., and S.R. Hart, Isotopic and incompatible element constraints on the genesis of island arc volcanics from Cold Bay and Amak Island, Aleutians, and implications for mantle structure, *Geochim. Cosmochim. Acta, 47*, 2015-2030, 1983.

Newman, S., J.D. MacDougall, and F.C. Finkel, ^{230}Th-^{238}U disequilibrium in island arcs: Evidence from the Aleutians and the Marianas, *Nature, 308*, 268-270, 1984.

Nichols, G.T., P.J. Wyllie, and C.R. Stern, Subduction zone melting of pelagic sediments constrained by melting experiments, *Nature, 371*, 785-788, 1994.

Pawley, A.R., and J.R. Holloway, Water sources for subduction zone volcanism: New experimental constraints, *Science, 260*, 664-667, 1993.

Peacock, S.M., Numerical Simulation of Subduction zone pressure-temperature-time paths: Constraints on fluid production and arc magmatism., *Philos. Trans. R. Soc. London, Ser. A, 335*, 341, 1991.

Pearce, J.A., Trace element characteristics of lavas from destructive plate boundaries, in *Andesites*, edited by R.S. Thorpe, pp. 525-548, John Wiley, New York, 1982.

Peccerillo, A., and S.R. Taylor, Geochemistry of Eocene calc-alkaline volcanic rocks from the Kastamonu area, northern Turkey, *Contrib. Mineral. Petrol., 58*, 63-81, 1976.

Piper, D.Z., Rare earth elements in ferromanganese nodules and other marine phases, *Geochim. Cosmochim. Acta, 38*, 1007-1022, 1974.

Plank, T., Mantle melting and crustal recycling in subduction zones, *Ph.D. thesis*, 250 pp., Columbia Univ., New York, 1993.

Plank, T., and C.H. Langmuir, An evaluation of the global variations in the major element chemistry of arc basalts, *Earth Planet. Sci. Lett., 90*, 349-370, 1988.

Plank, T., and C.H. Langmuir, Sediments melt and basaltic crust dehydrates at subduction zones, *EOS, Trans. AGU, 73*, 637, 1992.

Plank, T., and C H. Langmuir, Tracing trace elements from sediment input to volcanic output at subduction zones, *Nature, 362*, 799-742, 1993.

Plank, T., and J.N. Ludden, Geochemistry of sediment in the Argo Abyssal Plain at Site 765: a continent margin reference section for sediment recycling in subduction zones, *Proc. Ocean Drill. Program, Sci. Results, 123*, 167-189, 1992.

Plank, T., and W. White, Nb and Ta in arc and mid-ocean ridge basalts, *Eos Trans. AGU, 76 (46)*, Fall Meet. Suppl., 655, 1995.

Plank, T., T. Elliott, and W. White, Nb anomalies in arc lavas: insights from the Marianas, *Eos Trans. AGU, 75 (44)*, Fall Meet. Suppl., 730, 1994.

Poli, S., and M.W. Schmidt, H_2O transport and release in subduction zones: experimental constraints on basaltic and andesitic systems, *J. Geophys. Res., 100*, 22,299-22,314, 1995.

Potts, P.J., O.W. Thorpe, M.C. Issacs, and D.W. Wright, High-precision instrumental neutron-activation analysis of geological samples employing simultaneous counting with both planar and coaxial detectors, *Chem. Geol., 48*, 145-155, 1985.

Pratson, E.L., C. Broglia, A. Molinie, and L. Abrams, Geochemical well logs through Cenezoic and Mesozoic sediment from Sites 800, 801 and 802, *Proc. Ocean Drill. Program, Sci. Results, 129*, p635-6511992.

Reagan, M.K., and J.B. Gill, Coexisting calcalkaline and high niobium basalts from Turrialba volcano, Costa Rica: implications for residual titanates in arc magma sources, *J. Geophys. Res., 94*, 4619-4633, 1989.

Reagan, M.K., J.D. Morris, E.A. Herrstrom, and M.T. Murrell, Uranium series and beryllium isotopic evidence for an extended history of subduction modification of the mantle below Nicaragua, *Geochim. Cosmochim. Acta, 58*, 4199-4212, 1994.

Rhodes, J.M., Homogeneity of lava flows; chemical data for historic Mauna Loan eruptions, *Proc. Lunar Planet. Sci. Conf. 13th*, Part 2, *J. Geophys. Res., 88*, A869-A879, 1983.

Ringwood, A.E., The petrological evolution of island arc systems, *J. Geol. Soc. London, 130*, 183-204, 1974.

Ryan, J.G., I.J. Parkinson, and P. Austin, Boron and alkaline element systematics in diapiric serpentinites from ODP Leg 125: preliminary results, *Eos Trans. AGU, 74 (43)*, Fall Meet. Suppl., 675, 1993.

Ryerson, F.J., and E.B. Watson, Rutile saturation in magmas: implications for Ti-Nb-Ta depletion in island-arc basalts, *Earth Planet. Sci. Lett., 86*, 225-239, 1987.

Saunders, A.D., J. Tarney, and S.D. Weaver, Transverse geochemical variations across the Antarctic Peninsula: implications for the genesis of calc-alkaline magmas, *Earth Planet. Sci. Lett., 46*, 344-360, 1980.

Schiano, P., R. Clochiatti, N. Shimizu, R C. Maury, K.P. Jochum, and A.W. Hofmann, Hydrous, silica-rich melts in the subarc mantle and their relationship with erupted arc lavas, *Nature, 377*, 595-600, 1995.

Seno, T., The instantaneous rotation vector of the Philippine sea plate relative to the Eurasian plate, *Tectonophysics, 42*, 209-226, 1977.

Shaw, D.M., Trace element fractionation during anataxis, *Geochim. Cosmochim. Acta, 34*, 237-243, 1970.

Shipley, T.H , J.M. Whitman, F.K. Duennebier, and L.D. Petersen, Seismic stratigraphy and sedimentation history of the East Mariana Basin, western Pacific, *Earth Planet. Sci. Lett., 64*, 257-275, 1983.

Sigmarsson, O., M. Condomines, J.D. Morris, and R.S. Harmon, Uranium and ^{10}Be enrichments by fluids in Andean arc magmas, *Nature, 346*, 163-165, 1990.

Simkin, T., L. Siebert, L. McClelland, D. Bridge, C. Newhall, and J.H. Latter, *Volcanoes of the World*, 232 pp., Smithson. Inst., Stroudsburg, Pa., 1981.

Spiegelman, M., and D. McKenzie, Simple 2-D models for melt extraction at mid-ocean ridges and island arcs, *Earth Planet. Sci. Lett., 83*, 137-152, 1987.

Staudigel, H., K.-H. Park, M. Pringle, J.L. Rubenstone, W.H.F. Smith, and A. Zindler, The longevity of the south Pacific Isotope and thermal anomaly, *Earth Planet. Sci. Lett., 102*, 24-44, 1991.

Staudigel, H., G.R. Davies, S.R. Hart, K.M. Marchant, and B.M. Smith, Large-scale isotopic Sr, Nd, and O isotopic composition of altered oceanic crust at DSDP/ODP Sites 417/418, *Earth Planet. Sci. Lett., 130*, 169-185, 1995.

Stern, R.J., On the origin of andesite in the northern Mariana island arc: Implications from Agrigan, *Contrib. Mineral. Petrol., 68*, 207-219, 1979.

Stern, R.J., and L.D. Bibee, Esmeralda Bank: Geochemistry of an active submarine volcano in the Mariana Island arc, *Contrib. Mineral. Petrol., 86*, 159-169, 1984

Stern, R J., and E. Ito, Trace-element and isotopic constraints on the source of magmas in the active Volcano and Mariana island arcs, western Pacific, *J Volcanol. Geotherm. Res., 18*, 461-482, 1983.

Stern, R.J., S.H. Bloomer, P.-N. Lin, E. Ito, and J. Morris, Shoshonitic magmas in nascent arcs: New evidence from submarine volcanoes in the Northern Marianas, *Geology, 16*, 426-430, 1988.

Stern, R.J., J. Morris, S.H. Bloomer, and J.W. Hawkins, The source of the subduction component in convergent margin magmas: Trace element and radiogenic isotope evidence from Eocene boninites, Mariana forearc, *Geochim. Cosmochim. Acta, 55*, 1467-1481, 1991.

Stolper, E., and S. Newman, The role of water in the petrogenesis of the Mariana Trough magmas, *Earth Planet. Sci. Lett., 121*, 293-325, 1994.

Stolz, A.J., R. Varne, G.R. Davies, G.E. Wheller, and J.D. Foden, Magma source components in an arc-continent collision zone: The Flores-Lembata sector, Sunda arc, Indonesia, *Contrib. Mineral. Petrol., 105*, 585-601, 1990.

Stolz, A.J., K.P. Jochum, B. Spettel, and A.W. Hofmann, Fluid- and melt-related enrichment in the subarc mantle: evidence from Nb-Ta variations in island-arc basalts, *Geology, 24*, 587-590, 1996.

Sun, S.-s., and W.F. McDonough, Chemical and isotopic systematics of oceanic basalts: Implications for mantle composition and processes, in *Magmatism in the Ocean Basins*, pp. 313-345, edited by A.D. Saunders and M.J. Norry, Blackwell, Oxford, 1989.

Tatsumi, Y., Migration of fluid phases and genesis of basalt magmas in subduction zones, *J. Geophys. Res., 94*, 4697-4707, 1989.

Tatsumi, Y., D.L. Hamilton, and R.W. Nesbitt, Chemical characteristics of fluid phase released from a subducted lithosphere and origin of arc magmas: Evidence from high pressure experiments and natural rocks, *J Volcanol Geotherm. Res., 29*, 293-309, 1986.

Taylor, B., Rifting and the volcanic-tectonic evolution of the Izu-Bonin-Mariana arc, *Proc. Ocean Drill. Program, Sci. Results, 126*, 627-651, 1992.

Tera, F., L. Brown, J. Morris, I.S. Sacks, J. Klein, and R. Middleton, Sediment incorporation in island arc magmas: inferences from ^{10}Be, *Geochim. Cosmochim. Acta, 50*, 636-660, 1986.

Todt, W., R.A. Cliff, A. Hanser, and A.W. Hofmann, $^{202}Pb+^{205}Pb$ double spike for lead isotopic analysis, *Terra Cognita, 4*, 209, 1984.

Toyoda, K., Y. Nakamura, and A. Masuda, Rare earth elements of Pacific pelagic sediments, *Geochim. Cosmochim. Acta, 54*, 1093-1103, 1990.

Turner, S., C.J. Hawkesworth, P. van Calsteren, E. Heath, R. MacDonald, and S. Black, U-series isotopes and destructive plate margin magma genesis in the Lesser Antilles, *Earth Planet. Sci. Lett, 142*, 191-207, 1996.

Volpe, A.M., J.M. Macdougall, and J.W. Hawkins, Mariana Trough basalts (MTB): Trace element and Sr-Nd isotopic evidence for mixing between MORB-like and arc-like melts, *Earth Planet. Sci. Lett., 82*, 241-254, 1987.

von Heune, R., and D.W. Scholl, Observations at convergent margins concerning sediment subduction, subduction erosion and the growth of the continental crust, *Rev Geophys., 29*, 279-316, 1991.

Vroon, P.Z., M.J. van Bergen, G.J. Klaver, and W M. White, Strontium, neodymium and lead isotopic and trace-element signatures of the East Indonesian sediments: Provenance and implications for Banda Arc magma genesis, *Geochim. Cosmochim. Acta, 59*, 2573-2598, 1995.

White, W.M., and B. Dupré, Sediment subduction and magma genesis in the Lesser Antilles: Isotopic and trace element constraints, *J. Geophys. Res., 91*, 5927-5941, 1986.

White, W.M., and J. Patchett, Hf-Nd-Sr isotopes and incompatible element abundances in island arcs: Implications for magma origins and crust-mantle evolution, *Earth Planet. Sci. Lett., 67*, 167-185, 1984.

Wood, B.J., L.T. Bryndzia, and K.E. Johnson, Mantle oxidation state and its relationship to tectonic environment and fluid speciation, *Science, 248*, 338-345, 1990.

Woodhead, J., S. Eggins, and J. Gamble, High field strength and

transition element systematics in island arc and backarc basin basalts: Evidence for multi-phase melt extraction and a depleted mantle wedge, *Earth Planet. Sci. Lett., 114*, 491-504, 1993.

Woodhead, J.D., The origin of geochemical variations in Mariana lavas: A general model for petrogenesis in intra-oceanic island arcs?, *J. Petrol., 29*, 805-830, 1988.

Woodhead, J.D., Geochemistry of the Mariana arc (western Pacific): Source composition and processes, *Chem. Geol., 76*, 1-24, 1989.

Woodhead, J.D., and D. Fraser, Pb, Sr and Be isotopic studies of volcanic rocks from the northern Mariana islands: Implications for magma genesis and crustal recycling in the western Pacific, *Geochim. Cosmochim. Acta, 49*, 1925-1930, 1985.

Woodhead, J.D., R.S. Harmon, and D.G. Fraser, O, S, Sr and Pb isotope variations in volcanic rocks from the northern Mariana Islands: Implications for crustal recycling in intra-oceanic arcs, *Earth Planet. Sci. Lett., 83*, 39-52, 1987.

You, C.-F., P.R. Castillo, J.M. Gieskes, L.H. Chan, and A.J. Spivak, Trace element behaviour in hydrothermal experiments: Implications for fluid processes at shallow depths in subduction zones, *Earth Planet. Sci. Lett., 140*, 41-52, 1996.

B. Bourdon, Laboratoire de Géochimie et Cosmochimie, URA-CNRS 1758, IGPG, 4 Place Jussieu ,75252 Paris Cedex 05, France. (e-mail: bourdon@ipgp.jussieu.fr)

T. Elliott, Faculteit der Aardwetenschappen, Vrije Universiteit, de Boelelaan 1085, 1081 HV Amsterdam, Netherlands. (e-mail: ellt@mailhost.geo.vu.nl)

T. Plank, Department of Geology, 120 Lindley Hall, University of Kansas, Lawrence, KS 66045-2124. (e-mail: tplank@kuhub.cc.ukans.edu)

W. White, Department of Geological Sciences, Snee Hall, Cornell University, Ithaca, NY 14853. (e-mail: white@geology.geo.cornell.edu)

A. Zindler, National High Magnetic Field Laboratory, 1800 E. Paul Dirac Dr., Tallahassee, FL 32306-4005. (e-mail: zindler@magnet.fsu.edu)

(Received January 11, 1996; revised January 15, 1997;
accepted March 13, 1997.)